מכון ויצמן למדע
WEIZMANN INSTITUTE OF SCIENCE

Thesis for the degree

Master of Science

Submitted to the Scientific Council of the

Weizmann Institute of Science

עבודת גמר (תזה) לתואר

מוסמך למדעים

מוגשת למועצה המדעית של

מכון ויצמן למדע

By

Roy Patael Yohai

מאת

רועי פתאל יוחאי

מוות כתופעה קריטית ומגמות לא מונוטוניות במות שמרים תחת עקת חום

Cell death as a critical phenomenon and the non-monotonic patterns of death in yeast under heat shock

Advisor:

Prof. Roee Ozeri

מנחה:

פרופ' רועי עוזרי

Month and Year

March,2015

חודש ושנה עבריים

ניסן, תשעה

Abstract

The universality of critical phenomena, which lies in the mathematical field of Catastrophe Theory, has long been manifested beyond the scope of Physics with implications ranging from Ecology to Finance. In the field of Biology for example, there has been research studying critical aspects of cell population catastrophe [9]. In this research we examined a single cell as a complex system by itself, and asked: "**Is cell-death a critical phenomenon?**" This question lies in a broader context of the inquiry whether the relatively abrupt and irreversible phenomena of death is, in general, a manifestation of a complex system that is being pushed toward its tipping point.

To study our hypothesis we searched for two classic catastrophe flags: (1) a 'sudden jump' in the value of our state variable as a result of a small change induced on our control parameter. In our case this would correspond to a sharp transition between 'alive' and 'dead' as a function of some stress factor. (2) 'critical slowing down' which is the divergence of a typical time scale, close to a tipping point, following power-law scaling. Here, this would correspond to slowing down of death rates to a complete halt at the sharp transition point mentioned above.

The stress factor we chose to work with in order to kill cells was heat shock stress, due to its physical nature and the large literature and knowledge on heat shock mechanisms in cells. The cell model we chose was the Baker's yeast (Saccharomyces Cerevisiae) due to the large literature and previous studies on this cell model, as well as the many possibilities it offers in terms of genetic manipulations. In our research we accurately heated yeast in liquid medium to target temperatures using PCR thermo-cycler as a heating block. Following heating we determined the viable fraction by using the vital dye Propidium Iodide (PI) method. This stain is excluded from viable cells and stains only dead cells in red. By flow cytometry we were able to rapidly sample thousands of cells to reproducibly determine the viable fraction per temperature and heating time. We worked with low cell concentrations to reduce intracellular interactions.

Remarkably, the data we collected during the last year implies the presence of both desired catastrophe flags. Working with low temperature gradient for a long heating time of between 1-2 weeks, we witnessed the continuous decay of the viable fraction with

temperature (for a given heating time) change to an abrupt sigmoid shaped transition between viable (low) temperatures to non-viable (high) temperatures. In some cases the transition was as sharp as $0.6^0 C$. We measured slowing down of cell death rates with a critical exponent, $\gamma = -1.23 \left(-1.49,\ -0.98 \right)$, which might point out that the cell death process belongs to a universality class that is known to us from physics.

Measuring the viable fraction per temperature with high resolution, we discovered another interesting biological phenomenon which we extensively studied. We found out that, for a given heating time and for temperatures above the critical point, the viability level is not a monotonous function of temperature. Rather, we found local maxima where viability with exposure to higher temperature was higher than that of cells exposed to lower temperature, all other conditions being equal. This non-monotonic pattern repeats itself at different heating times, cell dilutions and temperature ranges, and is also reproducible in an outgrowth assay, with good agreement between the two methods.

We further linked this "viability salvage" with known components of the well-described heat shock machinery. We showed the crucial role of the stress response hubs msn2 and msn4 in the amplitude, timing and length of the salvage effect. Furthermore, we made first steps in linking activation of heat shock key players to appearance of salvage.

Contents

List of Abbreviations

BY4741- S288C derivative laboratory strain. Variation between the two is minuscule.

ESR - environmental stress response

HSP – heat shock protein

HSR- heat shock response

JUNQ - juxtanuclear compartment

PI – Propidium Iodide

RG – Renormalization group

S288C - A laboratory strain of Saccharomyces cerevisiae.

SC - Saccharomyces cerevisiae, the baker's yeast

SG - stress granule

STRE - 'stress-responsive element

UPS - ubiquitin-proteasome system

1. Introduction

1.1 Preliminary

The introduction to this thesis has two parts. The first describes the general broad aspects of critical phenomenon and the second overviews heat shock response in living cells. A more rigorous and mathematical review of critical transitions in the context of catastrophe theory and statistical mechanics can be found in the appendix.

1.2 Critical Phenomena

While our understanding of the basic building blocks in complex systems such as societies or eco-systems is rapidly expanding, we often understand very little of the mechanisms that determine major transitions and catastrophes in these systems such as the extinction of species or the outbreak of plagues. *Critical transitions theory* can arguably serve as a good framework for the description of such remarkable shifts often accompanying processes in complex, multivariable systems [40]. Understanding such transitions can open up surprising new ways to manage, manipulate and predict change.

In general, critical phenomena deals with the behavior of a system close to a tipping point (i.e. a critical point), where various universal characteristics are observed. As a simple example, suppose you are in a canoe and gradually lean farther and farther over to one side to look at something interesting underwater. Leaning over too far may cause you to capsize and end up in an alternative stable state: that of the canoe being upside down. Although the details of the theory of alternative stable states may appear tricky, several key properties can be seen in this simple example. For instance, returning from the capsized state requires more than just leaning a bit less to the side. It is difficult to see the tipping point approaching, as the position of the boat may change relatively little up until the critical tipping point. Close to the tipping point, resilience of the upright position is small, and minor disturbances such as a small wave can tip the balance. Also, if we pose the canoe closer and closer to its tipping point and let it recover, the time it takes the boat to return to its upright position grows larger and larger until it diverges at the critical point.

There has been a growing interest in the possibility of using generic statistical indicators, primarily based on *critical slowing down*, as early warning signals of impeding tipping points in various systems [1-8]. In catastrophes theory, critical slowing down refers to the slow recovery from small perturbations in the vicinity of the tipping point [1,10]. As the system approaches a tipping point the time needed to recover from perturbations becomes longer [4, 11], as illustrated by the canoe example.

1.2.1 Equilibrium in Dynamical Systems

The theory of *dynamical systems* is a branch of mathematics used to describe the time evolution of systems. One of its interests is equilibrium points, i.e. the points towards which a dissipative system tends to evolve to, and the stability properties of these special points.

An attractive way to depict the stability of a system is by means of a stability landscape as illustrated in Fig.1.2.1.1.The slope of the hills in the stability landscape corresponds to the rate of change in the system's state. At an equilibrium point the slope is zero, meaning that a system laid prepared in an equilibrium point will forever stay there if unperturbed.

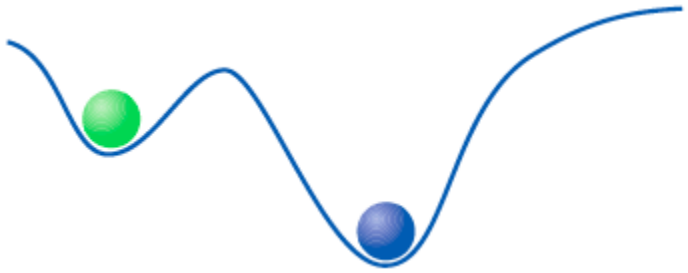

FIG 1.2.1.1 One can imagine the system like a ball settling in the lowest point, representing the equilibrium. This ''ball in a cup'' analogue is a good intuitive aid for grasping the essence of the matter. Two types of equilibrium points can be rightly observed: the unstable hilltop which is easily disturbed by external perturbations, and the bottom of a basin which will recover under small enough perturbations.

A *stable state* as depicted in these graphs is also called an *attractor*; systems can have several alternative attractors simultaneously. Different regions of the system state space, separated by sharp boundaries, will be attracted to different attractors. Generally

speaking, critical transitions happen when one attractor loses its stability and the system rolls to the next stable point.

1.2.2 Catastrophic Shifts and Bifurcation Points

The existence of multiple stable states can have profound implications for the way in which a system responds to changing conditions. Mostly, the equilibrium of a dynamical system moves smoothly in response to changes in the environment. Also, it is quite common that the system is rather insensitive over certain ranges of the external conditions. However, in some situations, one attractor loses its stability and a dynamic system abruptly falls into an alternative stable state. In that case, the curve that describes the response of the equilibrium to environmental conditions is typically ‘’folded’’ (Fig. 1.2.2.1). Note that such a *catastrophe fold* implies that indeed for a certain range of environmental conditions, the system has two *alternative stable states*, separated by an unstable equilibrium that marks the border (seperatrix) between the *basins of attraction* of the alternative stable states.

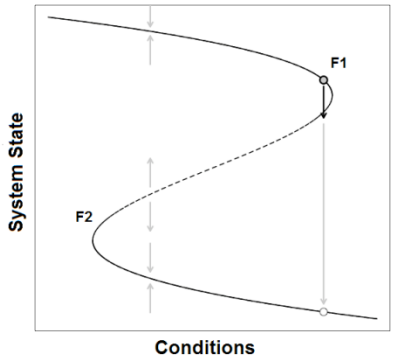

FIG 1.2.2.1 The equilibrium curve is folded backward, giving rise to three equilibria existing simultaneously for a given condition. The arrows in the graphs indicate the direction in which the system moves if it is not in equilibrium (that is, not on the curve which stands for the long term equilibrium states). Looking at the arrows’ directions it is easy to see that the bold line stands for stable equilibrium, while the dashed line points out at unstable equilibrium points.

We can now see why this situation is at the root of critical transitions. When the system is in a state on the upper branch of the folded curve, it cannot pass to the lower branch smoothly. Instead, when conditions change sufficiently to pass the threshold, a

‘’catastrophic’’ transition to the lower branch occurs (so called ‘forward shift’ while moving from lower to upper branch is termed ‘backward shift’). Clearly, this threshold is a very special point. In the jargon of dynamical systems theory, it is called a *bifurcation point*. Fold bifurcations are characterized by the fact that an infinitesimally small change in a control parameter (e.g. the temperature) can invoke a large change in the state of the system if it crosses the bifurcation point. Yet, another important feature is the fact that in order to induce a switch back to the upper branch, it is not sufficient to restore the environmental conditions from before the collapse. Instead, one needs to go back further, beyond the other switching point (F_1), where the system recovers by shifting back to the upper branch. This pattern, in which the forward and backward switches occur at different critical conditions, is known as *hysteresis*. From a practical point of view, hysteresis is important, as it implies that this kind of catastrophic transition is not easy to reverse.

1.2.3 Change in Conditions and Critical Slowing Down

Indeed, the idea of catastrophic transitions and hysteresis can be nicely illustrated by stability landscapes. To illustrate how stability is affected by changes in conditions, we create stability landscapes for different values of the conditioning factor (e.g. temperature) as demonstrated in Fig.1.2.3.1. For conditions at which there is only one stable state, the landscape has only one valley (see A, E curves). However, for the range of conditions where two alternative stable states exist (B-D), the situation becomes more interesting. The stable states occur as valleys, separated by a hilltop.

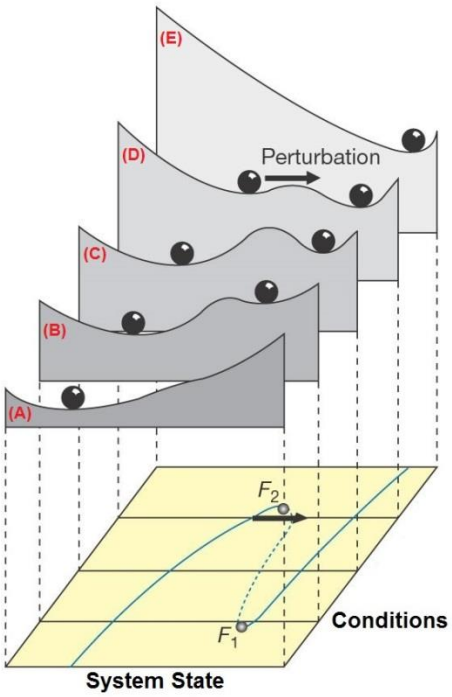

FIG 1.2.3.1 External conditions affect the resilience of multiple stable systems to perturbation. If the size of the basin of attraction is small (D), resilience is small, and even a moderate perturbation may bring the system into the alternative basin of attraction. Eventually, one attractor is losing stability (as in D→E or B→A) and the system suddenly remains with only one attractor point (e.g. A, E).

To illustrate catastrophic transitions imagine what happens when the initial conditions correspond to landscape A; the system will then be in the only existing equilibrium. Now suppose that conditions change gradually, so that the stability landscape changes to landscape B-D. Now there is an alternative attractor, but as long as no major perturbation occurs, the system will not move to this alternative attractor. If conditions change even further, the basin of attraction around the equilibrium in which the system rests disappears (as illustrated in E) implying a transition to the alternative state. Now if conditions are restored to previous levels, the system will not automatically shift back. Instead, it shows hysteresis. If no large perturbations occur, it will remain in the new state until the conditions are reversed beyond those of the landscape B.

Moreover, returning to landscape D were catastrophe transition occurs, we can see that the slope between the hilltop and the vanishing left valley tends to zero before becoming

the slope illustrated by landscape E. Hence, the characteristic rate with which the system will "role" to the next attractor will be very slow at this point. In fact, right at the critical point the typical time scale of the system would diverge. This phenomenon is called *critical slowing down*, and stands as a prominent fingerprint of a critical transition.

Let us take temperature to be our controlled condition upon which the landscape changes. Let us mark the temperature at which the critical transition takes place by T_c. As the temperature draws closer and closer to T_c the typical time grows, such that in the vicinity of the critical point it usually follows a power law scaling:

$$(T - T_c) \propto t_{char}^{\gamma} \qquad \textbf{(1.2.3.1)}$$

The *critical exponent* γ can be calculated for a specific system supplying us with an important characteristic of the system.

1.2.4 Universality

Generally speaking, universality is the observation that there are properties for a large class of systems that are independent of the specific microscopic details of the system. Systems display universality close to a tipping point, when a large number of interacting parts come together. This suggests that the most salient features of the critical transition (e.g. critical exponents' values) do not depend on the specific details of the system but rather on the broad class of dynamical systems to which it belongs.

As an important example, phase transitions in liquid-gas systems follow a critical exponent of $\gamma \cong 1.2 - 1.3$ which turns out to be quiet general, independent on the specific identity of the substances. Strikingly, this range is not unique to a liquid-gas system, as it manifests itself when describing magnetic systems, binary fluids and alloys, and other diverse, seemingly unrelated systems.

In Physics, the intriguing phenomenon according to which critical exponents take the same values for very different physical systems is called *universality*, and the group of phenomena that obeys the same critical values is called a *universality class*.

Much information can be gained when a process is attributed to a specific universality class, since some of these classes are well modeled and have been extensively studied (6.1.2).

1.3 Heat Shock Response

Cells grow optimally within a relatively narrow temperature range but tolerate moderate deviations, which affect cell structure and function, via rapid physiological adaptations. One of the most powerful adaptation mechanisms is the heat shock response (HSR), a highly conserved program of changes in gene expression that result in the repression of the protein biosynthetic capacity and the induction of a battery of cytoprotective genes encoding the heat shock proteins (HSPs). Many HSPs function as molecular chaperones to protect thermally damaged proteins from aggregation, unfold aggregated proteins, and refold damaged proteins or target them for efficient degradation. Much of what we know regarding the HSR in eukaryotic cells has been elucidated with the model yeast *Saccharomyces cerevisiae*.

1.3.1 Physiological and Metabolic Adaptation

1.3.1.1 Cell Cycle Arrest

Yeast cells complete a cell cycle by budding of a daughter cell in approximately 70 minutes in rich medium. Cells that activate HSR arrest their cell cycle in a point termed $G_{1;}$ at this point cells have not yet replicated their genetic material nor started budding a daughter cell. This arrest is transient in nature, and can be rapidly removed once conditions improve. By comparison, cells that experience starvation as a stress enter what is termed G_0 or quiescence. G_0 is a much more stable arrest of cell cycle. What is the competitive advantage of the G_1 arrest in response to protein misfolding? It is plausible that proceeding with DNA synthesis and/or mitosis in the face of proteotoxic damage might be catastrophic and that the G_1 delay allows protected time to restore protein homeostasis.

1.3.1.2 Metabolic Reprogramming

Starving cells that go into quiescence (G_0 phase) have been shown to be significantly more thermotolerant than exponentially dividing populations [12]. Several explanations

have been offered for the apparent heat resistance of starved cells, one of which focuses on the nonreducing disaccharide trehalose, an important storage carbohydrate in S. cerevisiae. The ability of cells to withstand severe heat shock (usually considered to be 45^0C or higher) correlates with cellular trehalose levels. The trehalose contribution to thermotolerance is probably due to the antidehydration role played by the disaccharides. It was demonstrated that trehalose can suppress the aggregation of misfolded proteins *in vivo*, effectively preventing one of the most deleterious consequences of severe heat shock [13,14]. The HSP104 protein chaperone possesses similar properties and works synergistically with trehalose to stabilize the yeast proteome at high temperatures. Indeed, both trehalose and HSP104 are required for tolerance to heat shock, suggesting that they play complementary but not overlapping roles [15, 16].

1.3.2 Protein Aggregation and Sequestration

The conventional view of heat shock stress is primarily one of proteotoxicity: an increase in the ambient temperature destabilizes cellular proteins. Lethality could then be predicted to result from misfolding and the subsequent loss of function of one or more essential proteins. Alternatively, the accumulation of a significant number of misfolded polypeptides could have secondary consequences, such as inhibition of normal protein degradation by the ubiquitin-proteasome system (UPS) or the formation of toxic protein aggregates. Both of these scenarios have been observed at lethal heat shock temperatures (>50^0C). Little is known about the state of the proteome at the more standard heat shock temperature for mesophilic yeast of 37^0C, where little to no protein misfolding is observed.

At standard heat shock temperature of 37^0C, the total fraction of proteins that is misfolded is not significantly altered. Maintenance of proteostasis under these conditions is done essentially by targeting misfolded proteins to either refolding by HSPs or to ubiquitination and degradation, mainly by the UPS [17]. The process of sorting misfolded proteins to the most appropriate fate involves aggregating them in specialized subcellular localizations. At 37^0C fluorescently tagged misfolded proteins accumulate in a juxtanuclear compartment (JUNQ). In JUNQ the misfolded proteins are segregated with the aim of refolding them either during or mainly after the heat stress resolves. If heat

shock is prolonged, misfolded substrates are observed in a second distinct compartment termed the IPOD (insoluble protein deposit), which exhibits a perivacuolar localization. Indications are that localization in IPOD indicates degradation as the final destination.

It is not clear if these compartments are intermediates in a normal protein quality control pathway or are off-pathway products. Lastly, the identification of these compartments provides an important link between the inclusion bodies of prokaryotes and the aggresomes of mammalian cells, all of which operate in thematically similar perhaps mechanistically distinct manners [18].

Interestingly, long-lived proteins are also damaged over time as cells age or in response to oxidative stress. Heat shock is known to induce oxidative stress. Protein oxidation frequently takes the form of the carbonylation of a number of amino acid side groups, resulting in the formation of irreversible semialdehydes [19]. Carbonylated proteins tend to form higher-order aggregates *in vivo*. Fascinatingly, these ‘’clumps’’ of damaged proteins are selectively retained in the mother cell during the asymmetric division of budding yeast [20]. This phenomenon likely contributes to the observed replicative senescence of yeast cells after 20 to 30 generations and to the finding that daughter cells are born free of damaged proteins. Further research on this clearly important process should help to shed some light on the issue, including the possibility that both random and nonrandom events may be in play.

1.3.3 Transcriptional Control of the Heat Shock Response

In addition to the physiological changes described above, cells respond to heat shock by dramatically altering their gene expression programs. For many years, analyses of the heat shock response occurred on a gene-by-gene basis, gradually describing a coordinated response orchestrated by a small number of transcription factors. Two studies documented the depth and breadth of what is termed the environmental stress response (ESR), including insults such as osmotic stress, salt stress etc. [21, 22]. Indeed, approximately 300 genes are induced in the ESR, and double that number, are transcriptionally repressed. Remarkably, the induction and repression of both gene classes are transient and scale with the magnitude (intensity) of the stress applied, demonstrating a reciprocal relationship [21, 22]. The HSR can be considered a subset of

the ESR, as essentially all HSR genes are accounted for within the ESR regulon, whereas a number of ESR genes are not necessarily induced by heat shock. The HSR is governed by the action of primarily two transcription factors, Hsf1 and the duo Msn2/4. Surprisingly, many of the genes induced by heat shock are not required for survival in heat; that is, the respective null mutants are not grossly heat shock sensitive [23]. A potential explanation is provided by the observation that the induction of the ESR/HSR is required not for survival of the stimulating stress but rather for survival of a subsequent stress. This phenomenon is termed ‘’acquired stress resistance’’ [24].

1.3.3.1 Chaperone Regulation

Early studies of cultured *Drosophila Melanogaster* cells showed that the expression levels of HSP genes increased rapidly after the initiation of heat shock, followed by a decrease in gene expression levels to slightly above baseline [25]. Substantial genetic and biochemical evidence suggests that two classes of heat shock proteins, HSP70 and HSP90, serve as trans-acting Hsf1 repressors. The HSP70/HSP90 chaperone complex represses the transcriptional activation of Hsf1 under nonstress conditions. During heat shock, the accumulation of unfolded or damaged proteins may divert the chaperone machinery away from Hsf1, thus allowing the derepression of the transcription factor.

1.3.3.2 Msn2/4

In addition to heat shock gene transcription mediated by Hsf1, a parallel pathway in S. *cerevisiae* senses and responds to a remarkable variety of other stresses. The regulatory element of this ‘’general’’ stress pathway was originally identified as an Hsf1-independent sequence in the promoters of the DNA damage-responsive gene DDR2 and the nutrient stress-responsive gene CTT1 [26, 27]. This ‘’stress-responsive element’’ (STRE)-mediated gene expression is mediated by two functionally related transcription factors, Msn2 and Msn4 [28].

The double deletion of *msn2* and *msn4* leads to sensitivity to thermal, oxidative and osmotic stresses [29, 30]. Of the two genes, Msn2 seems to play a more pronounced role. Genomic expression studies of yeast cells utilizing DNA microarrays revealed that the expression of MSN2 is constitutive under all conditions [22]. The multistress response

mediated by Msn2/4 is generally transient, governed by posttranslational modifications; the intensity and duration of the response are dependent on the level of the stresses [22].

1.3.4 Cross-Protection and Acquired Thermotolerance

The ability of cells to survive exposure to a sudden lethal temperature shock is defined as thermotolerance. Pretreatment at sublethal temperatures conditions cells to survive severe heat shock, which would otherwise be lethal.

The deletion of the inducible chaperone HSP104 dramatically decreased the transient thermotolerance conferred by a sublethal heat shock, suggesting that Hsp104 is one of the major components in that response [31]. In addition to cellular chaperons, levels of trehalose are also positively associated with thermotolerance. As opposed to HSP induction which is transient in nature, trehalose contribution to stress protection is long term [31]. Interestingly, the production of Hsp104 is regulated by both the heat shock transcription factor Hsf1 and the general stress transcription factors Msn2 and Msn4, while trehalose levels are modulated primarily by Msn2/4 [30]. Yeast cells exposed to sublethal stress gain tolerance not only to higher doses of the same stress but also to other disparate environmental stresses.

1.3.5 mRNA Sequestration in Response to Stress

Recent work has defined novel ribonucleoprotein assemblies, termed processing bodies (P bodies) and stress granules (SGs) that appear to concentrate nontranslating mRNAs in exchangeable but sequestered pools in response to a variety of stress conditions, including glucose starvation and osmotic stress. It is tempting to speculate that the formation of SGs may be yet another way for cells to reduce total protein synthesis under unfavorable protein-folding conditions such as heat shock. Moreover, a model wherein SGs act as temporary, protected ‘’storage’’ compartments for translatable mRNAs is attractive, as it would allow for the rapid reinitiation of the translation of existing transcripts when cells return to proliferative conditions. Such a model predicts that cells incapable of producing SGs in response to heat shock might exhibit reduced survival or delayed reentry into normal growth, but this hypothesis is yet to be tested.

1.3.6 Molecular Chaperones of the Cytoplasm

At any given time, hundreds of macromolecular processes involving proteins are occurring in the cytosol, so that protein-protein interactions must be governed and modulated appropriately [32]. In addition, the constant influx of newly synthesized polypeptides provides a significant protein-folding problem, as does the recognition of damaged proteins that must be targeted and shepherded for degradation. One way in which cells maintain the proper homeostatic balance of the proteome is through the activity of protein molecular chaperones. Molecular chaperones are a ubiquitous group of proteins involved in the folding and remodeling of other proteins [33]. Although the term ‘’heat shock protein’’ is commonly used synonymously with ‘’chaperone’’, distinctions must be made, as not all heat shock proteins are chaperones, and not all chaperones are induced by heat shock. Panoply of different classes of chaperones participates in protein biogenesis and quality control, and there is a growing appreciation that these machines cooperate in multichaperone networks.

1.3.6.1 The Hsp70 Chaperone System

The Hsp70 is arguably the most highly conserved family of proteins throughout evolution. In yeast, this ubiquitous family of chaperones is found in many cellular compartments and plays major roles in cell viability [34]. Hsp70s function primarily to ensure the proper folding of nascent or misfolded proteins through the recognition of determinants in the tertiary structure, usually the solvent exposure of hydrophobic patches normally buried within a properly folded protein.

1.3.6.2 The Hsp90 Chaperone System

Hsp90 is an evolutionarily conserved molecular chaperone unique in both function and client protein profile. In contrast to the Hsp70 chaperones, which recognize unfolded and misfolded proteins indiscriminately, Hsp90 functions primarily in the ‘’final’’ maturation of proteins and assembly of complex macromolecular structures. It also functionally interacts with a much more select group of substrates, termed ‘’client’’ proteins, which include many kinases and transcription factors.

1.3.6.3 Hsp104

Many stress conditions cause protein misfolding, and at high levels, this can lead to aggregation and cell death. The protein chaperone Hsp104 has the unique (in eukaryotes) capability of recognizing misfolded proteins within an aggregate and actively unfolding them, ultimately disassembling the insoluble structure and delivering substrates into refolding pathways.

Hsp104 is highly heat-inducible, nonessential protein in yeast, and deletion under optimal growth conditions does not impact growth [35, 36]. However, Hsp104 is required for thermotolerance, and the deletion of Hsp104 reduces cell survival 100-1000 fold [36]. In fact, increased levels of Hsp104 alone are sufficient to promote survival during lethal heat shock [35]. Hsp104 is unique among known protein chaperones in its ability to pull protein aggregates apart, leading to its characterization as a ‘’disaggregase’’.

Hsp104 is also a key player in prion inheritance. Hsp70 was also shown to be involved in Hsp104-mediated prion propagation and curing; although the exact role is unclear, it was proposed that the ratio between Hsp70 and Hsp104 could decide whether prions are cured or propagated.

1.3.7 Integral Feedback as a Simple Model for Biological Damage Response

The model proposed by [37, 38] showed that the heat shock systems are essentially integral feedback loops. In [39] the authors used a simple linear description of this feedback loop. A similar treatment will be presented in this part.

The integral feedback loop has three components. Environmental conditions u (i.e. thermal damage rate) cause a change in the system state y (e.g. temperature u causes increase in unfolded proteins y). The internal variable x acts to reverse the effect of the input, so that y returns to its baseline level (e.g. x are the HSPs that cause unfolded proteins y to return to a basal level). R is the repair rate factor which gives the probability of y re-folding when colliding with x, a HSP. Finally y_t stands for the proteome size (not including HSPs). We can then write:

$$\frac{dy(t)}{dt} = u(t)\cdot(y_t - y(t)) - Rx(t)y(t) \qquad \textbf{(1.3.7.1)}$$

Feedback in these systems occurs because an increase in y leads to production of x, causing y to return to its basal levels. Integral feedback is a specific form of feedback, in which the rate of production of x is dependent on the difference between the level of output y and its desired basal level y_0:

$$\frac{dx(t)}{dt} = k(y(t) - y_0) \qquad \textbf{(1.3.7.2)}$$

k corresponds to the responsiveness rate of x production, i.e. the gain of the integral feedback loop. The only possible steady-state for x is when $y = y_0$. For this reason, integral feedback is a robust circuit that eventually leads to the system state being equal to its target baseline, regardless of parameter values.

2. Goals

2.1 Catastrophe Flags' Observation

The universality of critical phenomena has long been manifested beyond the scope of Physics as its implications range from Ecology to Finance [40]. In the field of Biology, there has been research studying critical aspects of cell population catastrophe [9]. In this work we look at a single cell as a complex system by itself, and asked: "Is cell-death a critical phenomenon?" This question lies in a broader, fascinating context of the inquiry whether the relatively abrupt and irreversible phenomena of death in general is a manifestation of a complex system, with certain properties pushed toward its tipping point.

In particular, we wish to find evidence for critical slowing down when causing death in small microorganisms, and see if any bifurcation footprints can be observed.

2.2 Characterizing Dynamics of Thermal Death

Death of a cell is assumed to follow the exhaustion of homeostatic capacity in the face of ongoing stress. In the case of thermal stress, the homeostatic machinery is provided by the heat shock response, thus delaying death. However, the interplay between the extent of stress, the presence of a homeostatic response and death has not been previously studied.

If the heat stress load is generally composed of temperature and heating time, we wanted to map the whole landscape of possible combinations of both, and measure the corresponding viability percentage.

Early in the research we found that under certain conditions, for a given heating time, viability level is not a monotonous function of temperature; we focused much of our efforts trying to understand this intriguing phenomenon.

3. Methods and Materials

3.1 Materials

Yeast strains used in this study are derived from S288c or BY4741 background strains or taken from the GFP library (Huh et al., 2003) as listed below.

Table 3.1.1

BY4741	**MATa {his3Δ1 leu2Δ0 met15Δ0 ura3Δ0}**	
YMS2218	MATa *Δmsn2*::pFA6a-NAT-MX6	This study
YMS2219	MATa *Δmsn4*::pFA6a-NAT-MX6	This study
YMS2250	MATa HSF1-OE::Ura	This Study
YMS1621	MATa 4xHSE-emerald GFP::URA	J. Weismann
GFP library	MATa HSP104::pFA6a–GFP(S65T)–His3MX	
S288c	**MATα {SUC2 gal2 mal mel gal2 CUP1 flo1 flo8-1}**	**ATCC**

Propidium iodide (Sigma, UK) was dissolved in PBS at a concentration of 0.2M. This stock solution was stored at -20°C and on the day of experiment the stock was diluted in PBS and then mixed 10:1 with yeast suspension diluted in PBS as well to OD 0.3, to give a final PI concentration of 2mM per 0.03OD/ml of yeast. Samples were incubated at room temperature in the dark for 20 min prior to analysis. Flow cytometry analyses were performed using a BD LSR-II flow cytometer. The forward scatter and side scatter signals from the Argon ion (488nm) laser were used to discriminate the cells of interest from the debris and background noise. The PI fluorescence was collected via a 630nm band pass filter. Cells in log growth and heat killed cells (70^0C, 15 minutes) were used as live and dead controls respectively to verify grouping of cells as PI negative or positive. Total cell counts per group were obtained from the PI histogram.

3.2 Experimental Methods

3.2.1 Sample Preparation

We prepared a starter of our sample strain in YPD and placed it in a 30^0C centrifuge overnight. We then diluted the sample to SD-complete by the right amount, yielding a 0.2-0.8 OD (exponential growth phase) after overnight centrifugation.

In the case of water-medium experiments we centrifuged the cells (3000 rcf for 3 minutes in 25^0C), then sucked the SD-complete medium and replaced it with water. After 1 hour in 30^0C centrifugation we diluted the sample to the desired OD ($\cong 0.25$).

3.2.2 PCR thermo-cycler as a Heating Block

We used a PCR thermo-cycler as a heating block. Each sample of yeast is divided between tubes; each tube is exposed to constant temperature, and sampled on consecutive timepoints.

3.2.3 Vital Staining by Propidium Iodide

For read out in plate format, we applied vital staining by Propidium Iodide [41], which is a red die binding to nucleic acids, allowing us to see dead cells staining with red and viable cells as unstained, namely, PI negative.

We dilute 1:90 a desired measure of the $PI \times 100$ stock in PBS to get our final staining medium. Working with 96-well plate, we distribute 90µl of the medium in each well we are about to measure. From this step forward, special care is given to prevent the plate from light exposure.

Once heat shock protocol has ended 10µl of the heat shocked solution are immersed in each well of the pre-prepared 90µl PI-wells.

Finally, the plate is placed in a shaker calibrated to ~700 rpm for half an hour, at the end of which the plate is taken for cytometry measurement.

3.2.4 Flow Cytometry

Values were set so at least 90% of the cells can be included in a size gate determined by FSC-SSC scatter plot. Borders between viable and dead cells were determined by a histogram of PI intensity, as calibrated by positive (30^0C for 15 minutes) and negative (70^0C for 15 minutes) controls of cells in exponential growth.

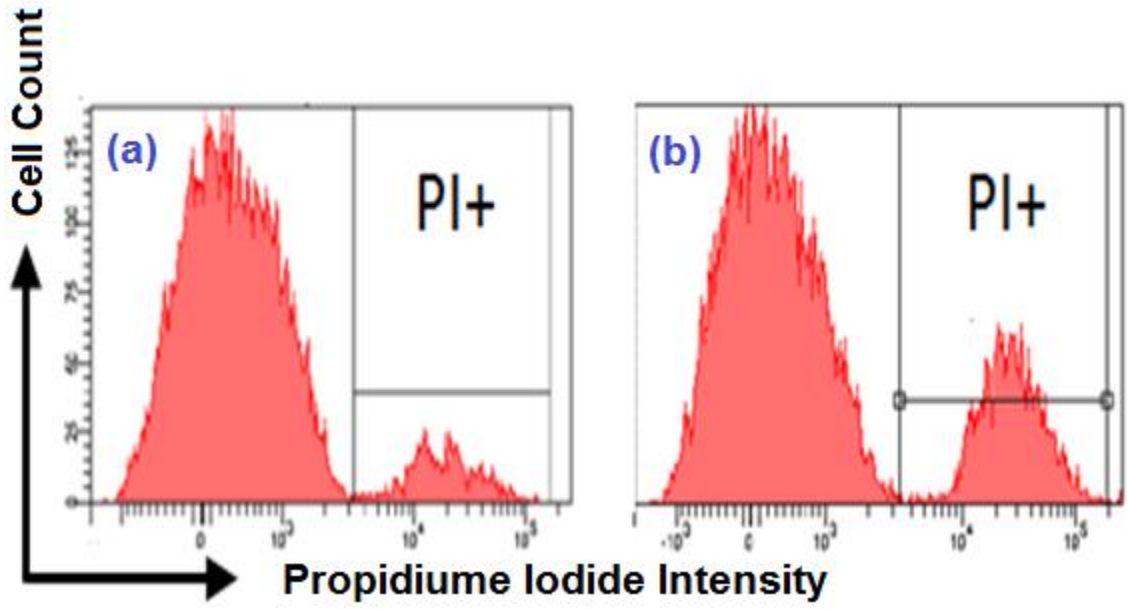

FIG 3.2.4.1 Flow cytometry distributions for live/dead control experiments. (a) Cell count distribution for a live control experiment in which cells were heated for 15 minutes at 30^0C. (b) Cell count distribution for a dead control experiment in which cells were heated for 15 minutes at 70^0C.

We work in 'throughout' mode and determine the following technical parameters:

Table 3.2.4.1	
Sample flow rate	1µl/sec
Sample volume	90µl
Mixing volume	50µl
Mixing speed	200
Number of mixes	2
Wash volume	400µl

A typical sample size will be 4,000 cells.

4 Results

4.1 Bifurcation and Critical Slowing Down

All the measurements described in this part were conducted in a water medium to prevent cell proliferation under mild heat shock during long extended heating times.

4.1.1 Identification of the critical point

Heating the samples for short (less than a day) and intermediate (less than a week) time lapses, one can find a continuous decay pattern as illustrated in Fig. 4.1.1.1. The filled circles are the averages of 2-3 measurements whereas the error bars represent one standard deviation. Solid lines are generated following an interpolant fit to a polynomial function (i.e. a smoothing spline) and are shown as a guide to the eye only

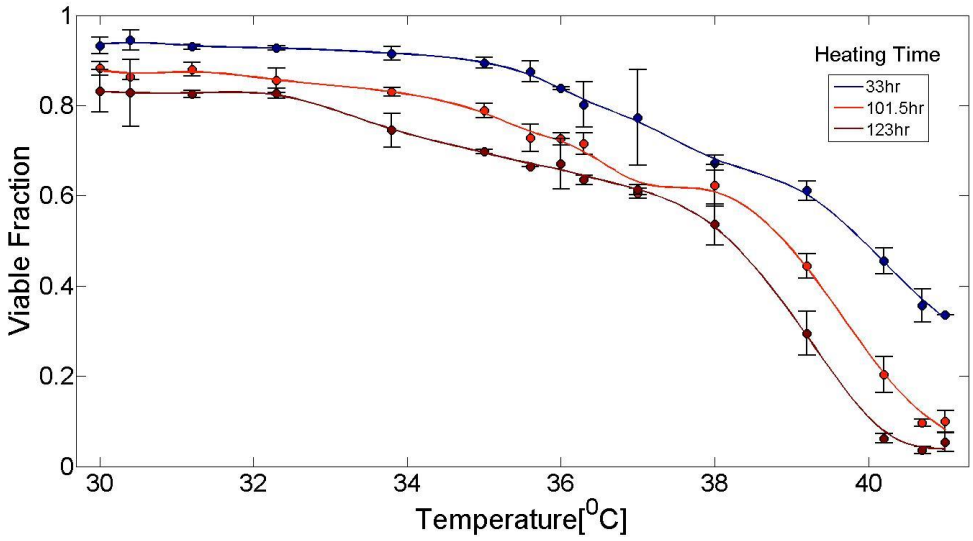

FIG 4.1.1.1 Viability levels for different intermediate heating times follow a continuous decay pattern. The filled circles are the average result of 2-3measurements and the error bars are one standard deviation. Solid lines are generated following an interpolant fit to a polynomial function (i.e. a smoothing spline) and are shown as a guide to the eye only. A kink is created as heating time is increased.

Viability levels remain more or less independent of temperature until 35^0C where the viable fraction begins to drop with increasing temperatures.

However, at longer heating times we observed a clear change of behavior, as the relatively gradual decay cleared the way to a sharp sigmoidal decay pattern (see the red curve in Fig. 4.1.1.2). After a heating time of 167 hours, viability collapses by 70% across a change of roughly 0.6^0C. This data supports the identification of 35^0C as a candidate for a critical temperature, below which cells are able to remain viable with good probability (>70%) even after long heating times, whereas at temperatures slightly above the critical temperature survival probability tends to zero.

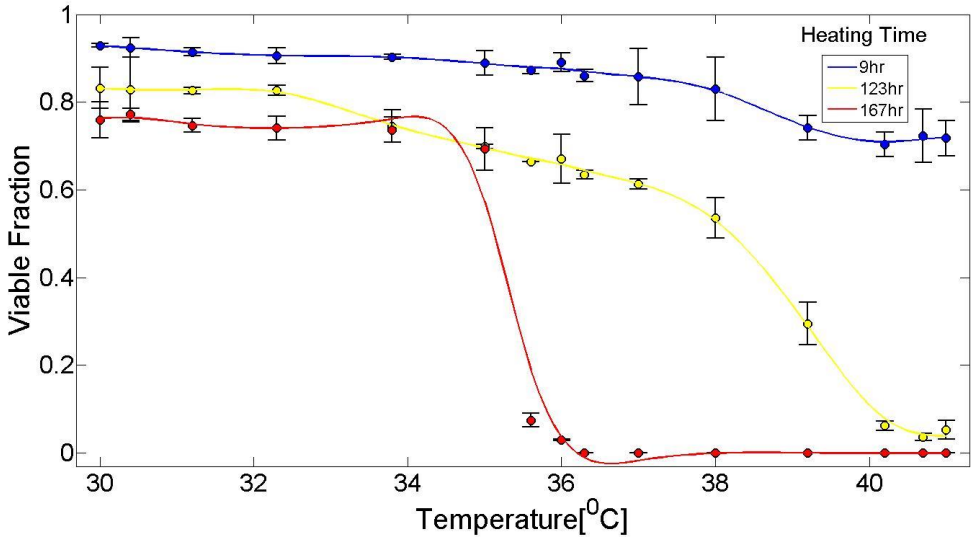

FIG 4.1.1.2 viability vs. temperature for short (blue, 9 hrs), intermediate (yellow, 123 hrs) and long (red, 167 hrs) heating times. After 167hrs of heating viability levels collapse at temperatures higher than 35^0C with a slope that is at least as sharp as 0.6 degrees.

Since the heating time and temperature form a 2D parameter space, a 2D surface can be rendered which shows the different behavior domains in one graph (Fig. 4.1.1.2). The point of collapse slightly drifts toward lower temperatures from 35^0C to 33^0C as heating time varies from 167 hrs to 316hrs. However, at 316 hrs of heating we observe thermal death below 33^0C as well, suggesting that the critical temperature is at lower temperatures still. This regime of lower temperatures and very long heating times is currently under investigation.

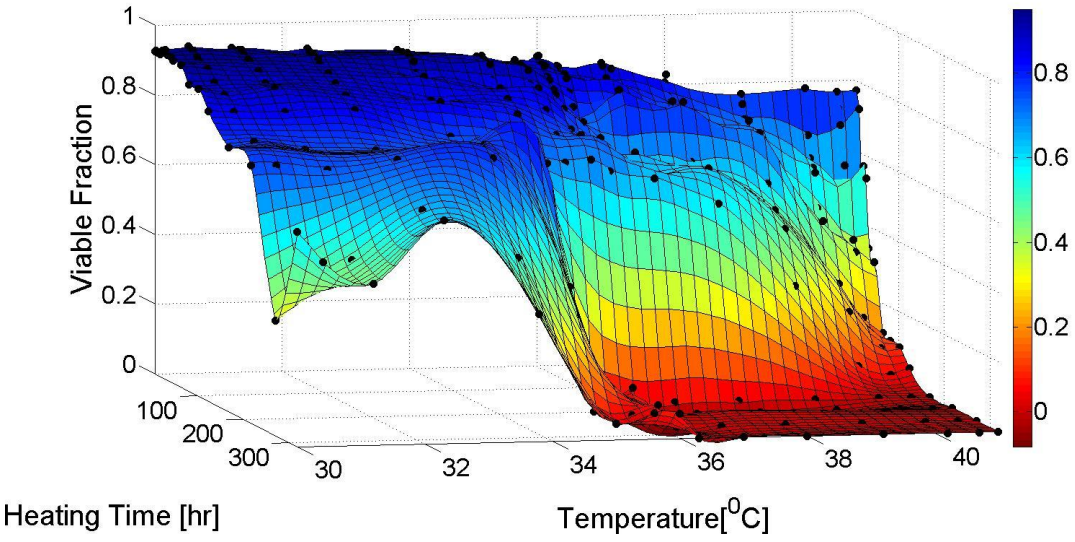

FIG 4.1.1.2 Viability surface in the time-temperature parameter space. Continuous viability decay with temperature is replaced by sigmoidal shaped curves at long heating times. Sigmoidal viability decay is traced to heating times as long as 316hr (last measurement in this specific session).

4.1.2 Critical Slowing Down

The data shown in the last section supports the existence of a bifurcation where above a critical temperature of 32 C at sufficiently long times the yeast cells are bound to eventually die. In critical phenomena, the transition rate from one attractor to the other slows down following a power-law as one approaches the critical point. Here, we take a critical temperature of $T_c = 32.3^0 C$ and use the half-life time of the viability at different temperatures as a measure of the inverse rate. A more thorough approach would have been to fit our data to a functional decay curve and thus extract the decay rate (as an example, a constant rate would lead to an exponential decay curve). However, in this case, we observe different time curves at different temperatures that vary from exponential like decay at higher temperatures to a sigmoidal decay as one approaches the critical temperature. We fit our data to a power law behavior, $t1/2 = a \cdot (T - Tc)^b$ where b is a critical exponent. The results are plotted in Fig. 4.1.2.1. The data fits relatively well with power-law slowing down and the critical exponent we calculated is

$b = -1.23\ \left(-1.49,\ -0.98\right)$. This critical exponent is typical to many critical systems in physics.

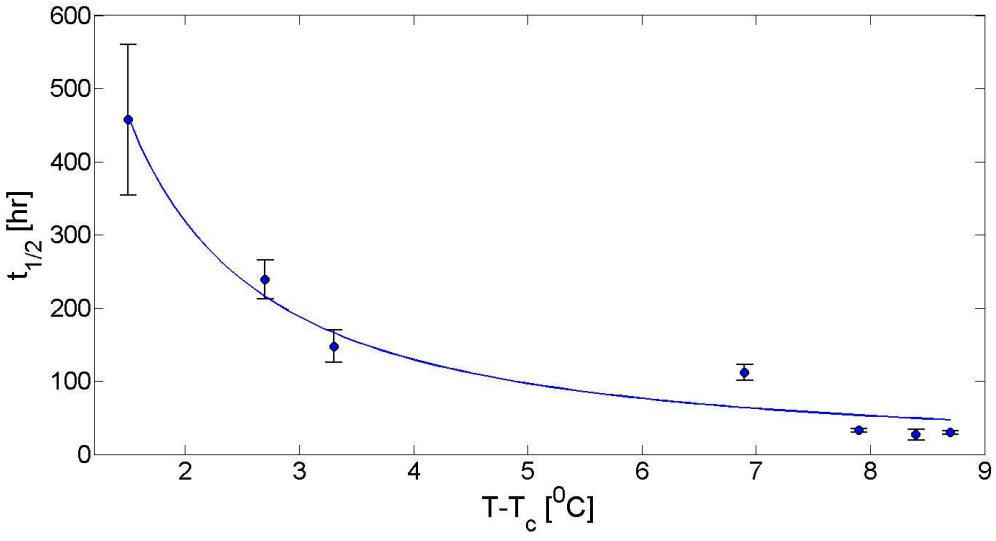

FIG 4.1.2.1 Half-life viability decay times vs. temperature. $R^2 = 0.988$. The blue solid line is a maximum likelihood fit of a power law decay $t1/2 = a \cdot (T - Tc)^b$. We measure a critical exponent value of $b = -1.23\ \left(-1.49,\ -0.98\right)$ which corresponds with a well-known physical universality class.

Since critical behavior manifests itself in the neighborhood of a critical point, one may choose to work only within a 4^0C interval from the critical temperature where the typical time-curves are sigmoidal shaped. The results however are almost identical in both cases.

4.2 The Induction of a Salvage Mechanism during Heat Stress

All the measurements described in this part were conducted in SD medium. When heating yeast in SD medium a qualitatively different behavior was observed. Here, instead of a monotonous decay in viability probability with rising temperature, we have found that for some heating times viability shows non-monotonicity vs. temperature.

4.2.1 Non-Monotonic Viability Curves

Measuring the viability levels in the 50^0C - 56^0C temperature interval we found that a non-monotonous curve links viability with heating, so that for a given heating time, heating to higher temperatures is significantly less detrimental than slightly lower ones, as illustrated in Fig. 4.2.1.1:

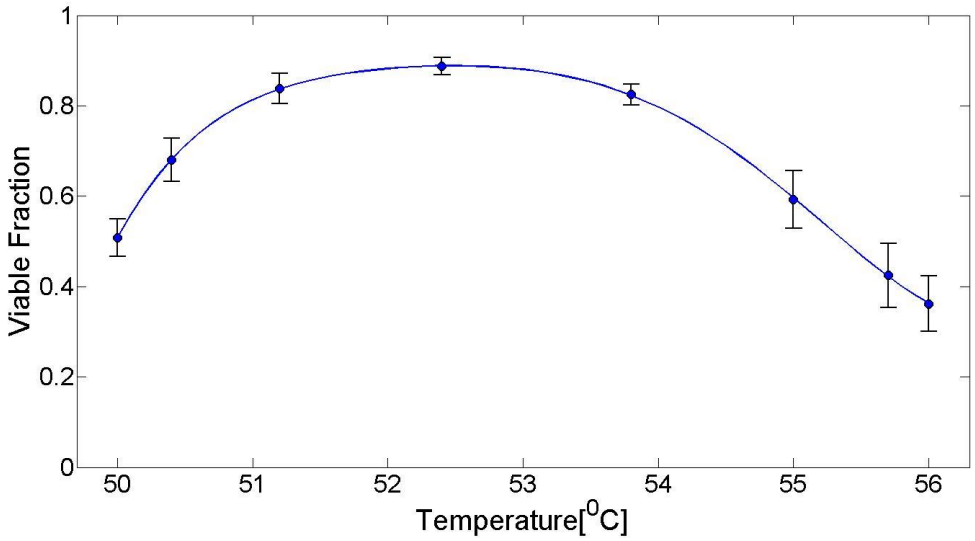

FIG 4.2.1.1 Viable fraction vs. temperature. Heating time was set to 45 minutes. The blue solid line is a polynomial fit and is provided as a guide to the eye. The surprising part of the figure is the positive slope below 52 C. This positive slope indicates that, in this temperature range, the survival probability of cells increases with temperature.

We identified that this "salvage" pattern is repetitive, unveiling in different temperature ranges at different times.

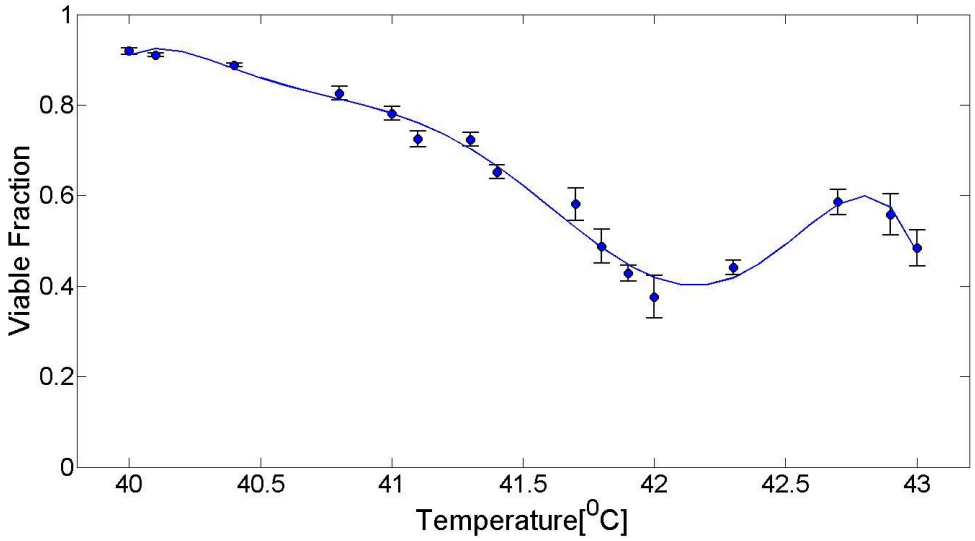

FIG 4.2.1.2 Viable fraction as a function of temperature. Another 'salvage point' (i.e. maximal viability point) is seen at 42.7^{0}C after 11 hours of heating.

To get the whole picture we calculated the half life time of yeast for the 37^{0}C – 56^{0}C temperature interval with a characteristic temperature resolution of less than one degree. The viability half-lives at different temperatures are shown by the filled circles in Fig. 4.2.1.3 on a semi-log scale. The half-life times decrease exponentially with increased temperature with the exception of a couple peaks of increased times around 42^{0}C and 52^{0}C.

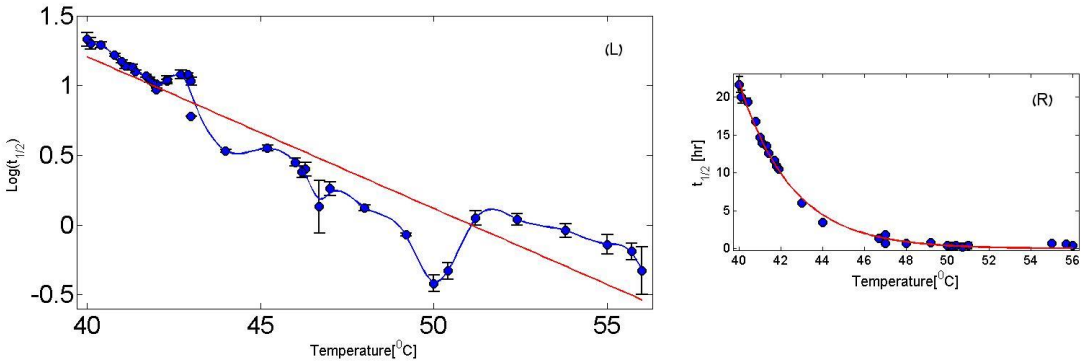

FIG 4.2.1.3 Half-life vs. temperature graphs. Red solid lines are exponential fit to the data with the peaks removed as shown by the right figure. While the overall trend is an exponential decrease with temperature, two salvage peaks appear, as illustrated on the left figure.

Interestingly, these peaks of prolonged viability completely vanish when working with a water medium instead of SD, as illustrated in Fig. 4.2.1.4. Following the sample's centrifugation, SD medium was vacuumed and replaced by distilled water. After 1 hour in water we followed the usual heat shock protocol. The fact that the peaks of non-monotonous viability half-life disappear in water may hint towards a connection with the proliferation of yeast which also disappears in water.

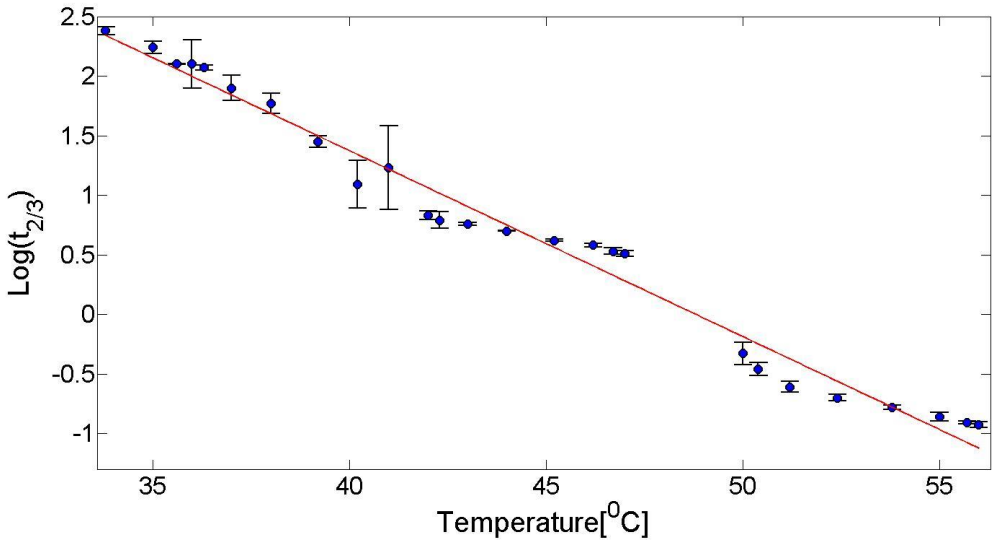

FIG 4.2.1.4 Viability Log (t2/3) vs. temperature in water medium. The typical times follow an exponential decrease without any non-monotonous behavior such as that observed in SD.

4.2.2 A Dynamic Salvage Pattern

So far, the time dynamics has been displayed using a single number per temperature, i.e. the viability half-life time. Further understanding can be gained by studying the full behavior of viability vs. time and temperature. Fig. 4.2.2.1 shows the viable fraction for different heating times and temperatures ranging from 50^0C to 56^0C. Fig. 4.2.2.2 shows the same data with a polynomial 2D surface fitted to the data. As seen in the figure, the maximum viability peak temperature is decreasing as the heating times are prolonged. This behavior is manifested by the diagonal "ridge" in the 2D surface shown in Fig. 4.2.2.2.

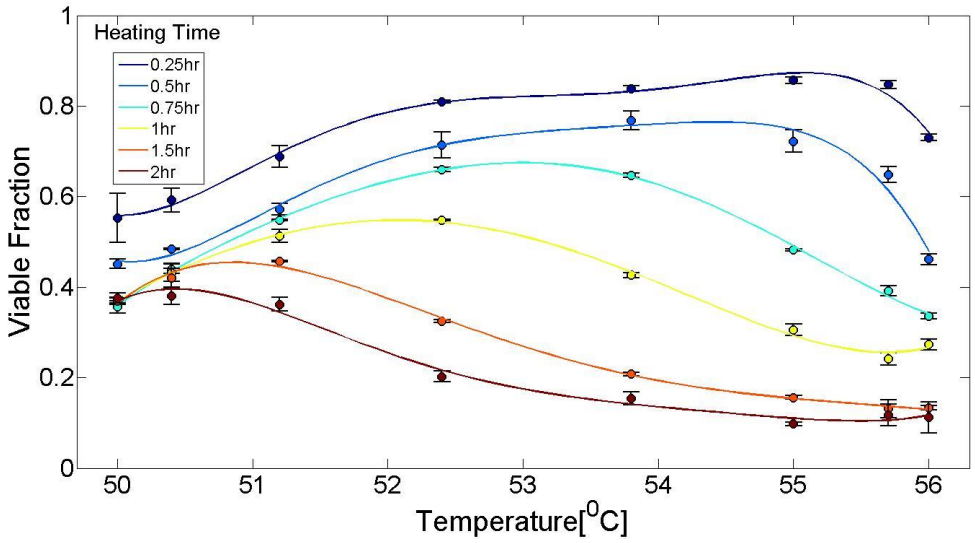

FIG 4.2.2.1 Viable fraction for different heating times vs. temperature. The salvage point drifts toward lower temperatures as heating time is increased.

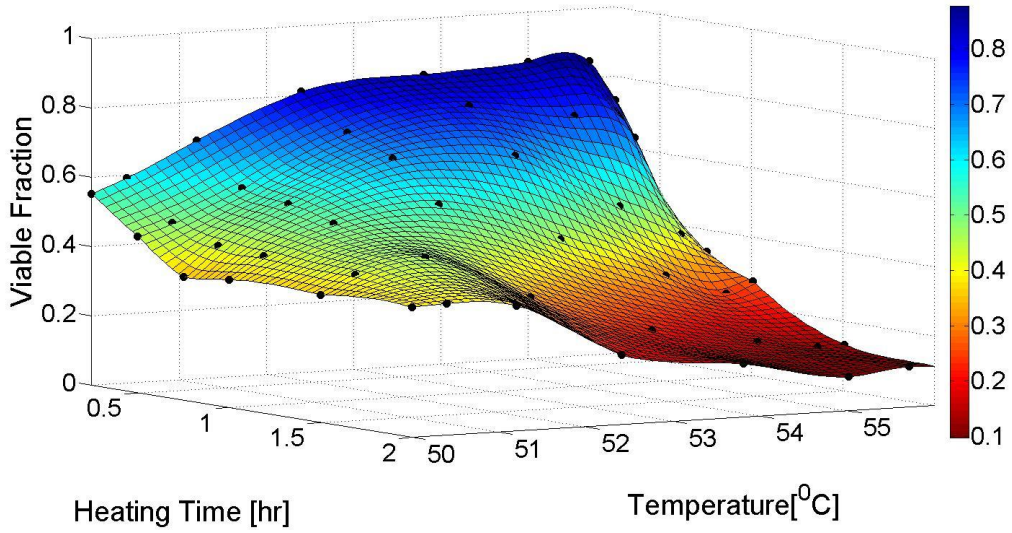

FIG 4.2.2.2 Viability surface in the time-temperature parameter space. The salvage effect is traced to the left side of this 2D manifold where increased temperature ends up with higher viability levels. The diagonal ridge depicts the dynamic nature of the salvage effect in the 50^0C – 56^0C temperature interval.

4.2.3 O.D recovery times follow salvage lead

As a cross-check we examined the proliferation rate of yeast cells following the same heat shock. A repetition of the salvage patterns in the recovery rate would help rule out systematic effects in flow cytometry viability measurements. It would also link the survival strategy of yeast cells activating their HSM to their post-heat shock proliferation and therefore also to a possible evolutionary explanation. Following heat shock the yeast were retained in SD medium at 30^0 C for a variable amount of time. The OD of the sample was then measured as a measure of the yeast increase of population.

The results we got are shown in Fig. 4.2.3.1-L. Here different temperatures between 41.5^0C – 44.5^0C were applied to yeast in SD medium for a time of 14 hours. The OD of the post heat-shock samples vs. time is shown by the different solid lines. In the right figure (red line) we can see that the recovery rate (calculated as the rate at which a sample reached a half-saturation level, i.e. OD=0.27) follows similar non-monotonous trend as the viability salvage pattern (blue line) described previously, thus reassuring previous results.

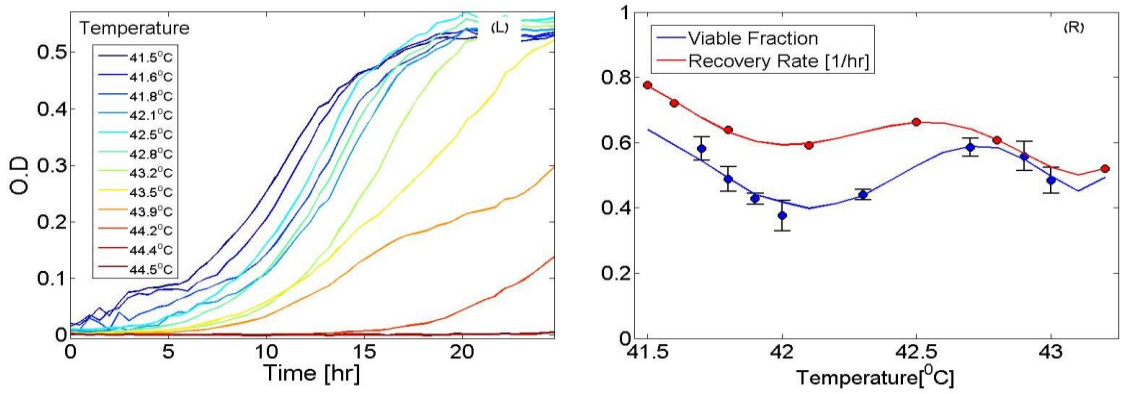

FIG 4.2.3.1 (L) O.D levels as a function of time following a 14 hours heat-shock protocol. Colors (i.e. temperatures) are not monotonically ordered. (R) A comparison between salvage in viability levels following an 11 hours heat shock protocol (blue line) and recovery rates (red line). Recovery rates were calculated as the rate at which a sample reaches half-saturation levels, (OD=0.27), and were normalized in order to have a compatible y-scale for both curves. It is clear that the salvage pattern repeats itself in the O.D recovery picture, standing in good agreement with the viability salvage picture.

Moreover, the O.D recovery picture shows us in a clear way the asymmetry between the temperatures before and after the salvage peak. After heating the cells for 14 hours, viability levels before and after the maximum viability temperature of 42.7^0C are symmetric, i.e. there is no difference between lower and higher temperatures around the maximum. However, as seen in Fig. 4.2.3.1-L the recovery rates follow very different behavior on both sides of the salvage point. Recovery after a heat shock of 42.5^0C is much faster than recovery at 43.5^0C. This observation suggests that although the same number of yeast cells survived, their ability to divide has been compromised by the stress. This could be due to the depletion of resources by the HSM that was required in order to survive severe ongoing stress.

4.2.4 Cell division salvage pattern

The next question we wanted to answer was: what is the role cell proliferation during the heat shock itself plays in the viability pattern observed. To this end we measured OD levels during heat shock. Here, we used a heat bath as a heating device instead of the PCR thermos-cycler. O.D levels were measured on consecutive time points. The discrete temperature points were selected around the viability peak apparent in Fig. 4.2.1.2. As can be seen in Fig. 4.2.4.1, the O.D levels reproduce the non-monotonous behavior introduced in previous sections. The 42.7^0C temperature, which is a maximum viability point, turns to be a minimum OD point for all measured times (6-17hr). Moreover, the non-monotonous OD pattern not only switches polarity (a maximum becomes a minimum), but also appears as early as 6 hours heating, preceding the viability peak which only appears after 11 hours. These results imply that cell division rates may play a crucial role in the salvage pattern production.

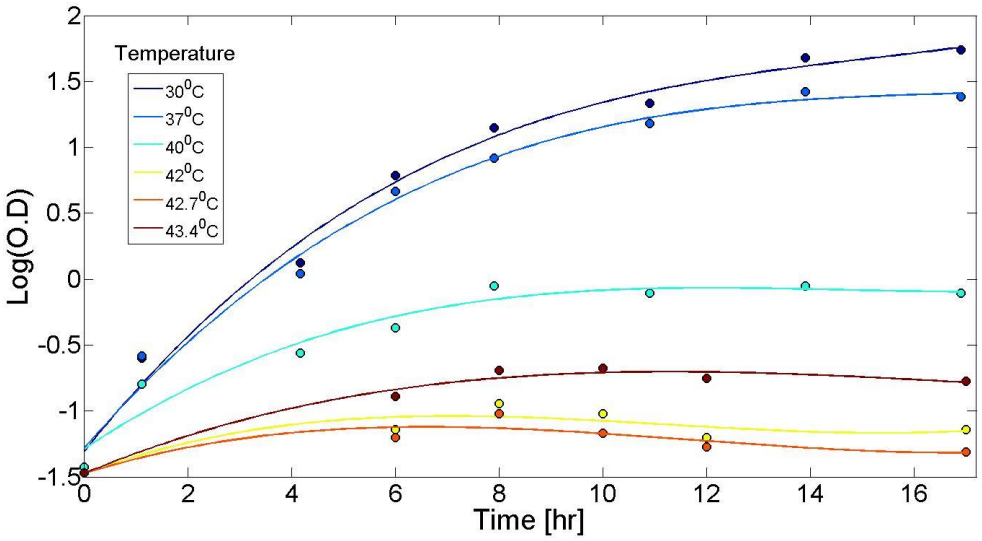

FIG 4.2.4.1 OD levels during a heat shock stress. The 43.4^0C curve is posed over the 42^0C and 42.7^0C curves for all measured times.

Fig. 4.2.5.2 compares between the non-monotonous pattern in viability levels and in O.D values vs. different heating times for 42^0C and 43^0C. As seen, the proliferation rate at 43.4^0C is higher than in 42^0C for all heating times. However, the viability levels at 42^0C are higher than 43^0C for heating times shorter than 10 hours after which the survival probability at 43^0C is higher. This is an indication that the higher proliferation rate at 43.4^0C is not the only mechanism behind increased viability. It is possible however that cell division serves as a HSM of some sort, perhaps through the release of damaged proteome in the mother cell. This observation is also consistent with the absence of non-monotonous salvage patterns in water solution.

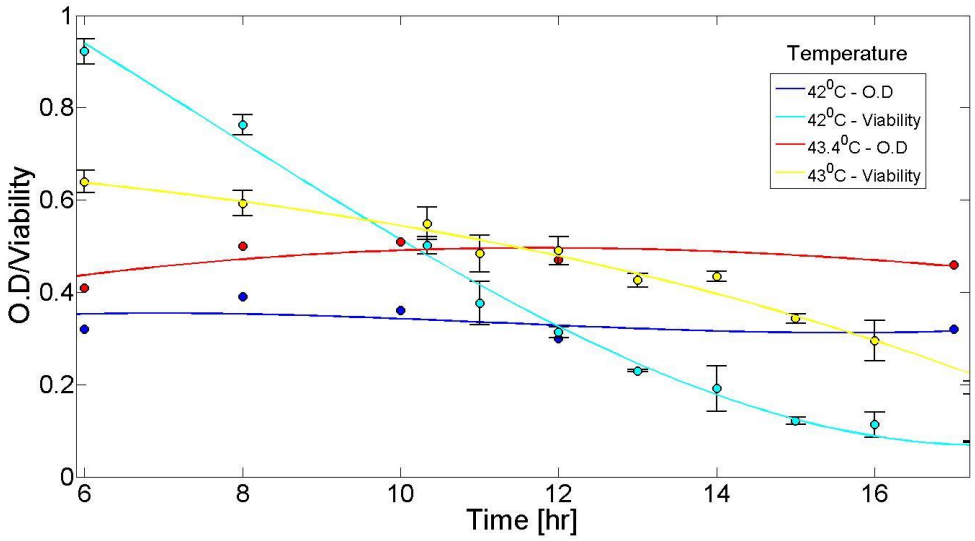

FIG 4.2.4.2 OD and viability levels during a heat shock stress. In short heating times (until ~10 hours) we see a higher division rate in the higher temperature, whereas the higher viability levels are traced to the lower temperature. In long heating times both O.D and viability levels are higher at higher temperatures.

4.2.5 Knockout Protocol

In this part we examined the response to heat stress of cells in which some of the heat shock machinery was genetically inhibited. As a first measurement we used $\Delta msn2$. As mentioned in the introduction, *msn*2 is a transcription factor mediates the stress-responsive element of a ''general'' stress pathway. Fig. 4.2.5.1 compares viability levels of the regular yeast we use (BY4741) and the modified $\Delta msn2$. The deletion of *msn*2 turns out to be significant when dealing with temperatures close to the salvage point, supplying us with evidence to the role of the HSM in the creation of a viability salvage pattern. However, the more striking part of this figure is the viability of $\Delta msn2$ in the low viability temperature (~41.7^0C) of BY4741. At this temperature, the viability levels of $\Delta msn2$ are higher, indicating that under these stress conditions it is beneficial to inhibit *msn*2 activity in the stress response. This surprising behavior was also observed with the O.D recovery protocol described on section 4.2.3, with a good correlation.

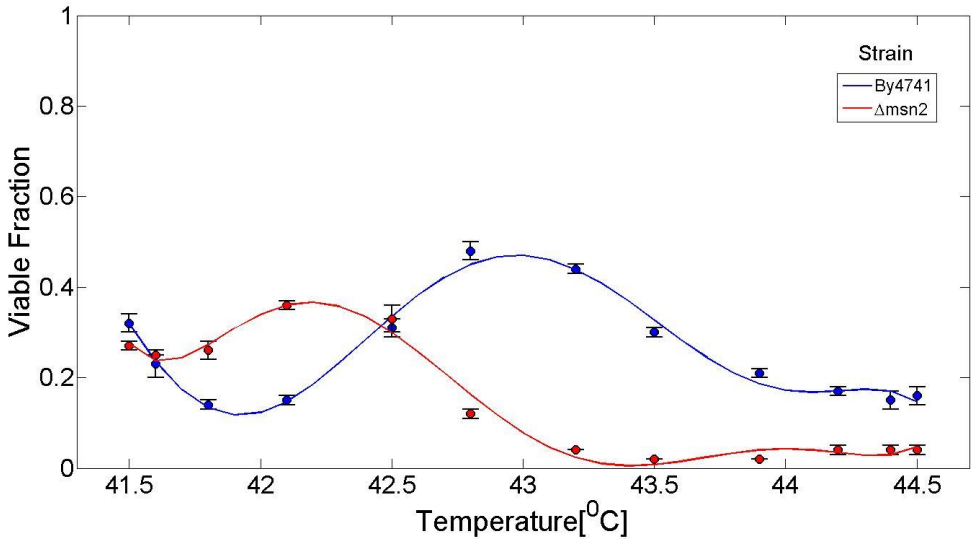

FIG 4.2.5.1 Viability levels of BY4741 and Δ*msn*2 after 14 hours of heating. The sinusoidal pattern in Δ*msn*2 is shifted leftward with respect to the salvage peak of BY4741. The most surprising part however lies in the deep (~42^{0}C) preceding the salvage peak, where the red curve describing Δ*msn*2 is on top of the blue curve describing the wild type strain.

4.3 A Suggested dynamical model

The response of the cell to heat stress has been previously modeled using linear differential equations that describe the operation of the feedback mechanism that is involved, as detailed in sec. 1.3.7. Here we extended this model in two ways. First, we included non-linear terms in the equations to allow the failure of the feedback mechanism at increased stress. The non-linearity introduces a bifurcation and critical behavior into the heat shock dynamics. Secondly, to relate the outcome of the model to the results of our experiments which are probabilistic in nature, i.e. measure survival probability, we introduced stochasticity into the equations. This is, to our knowledge, the first description of the heat shock response and thermal death of a cell through non-linear stochastic differential equations.

4.3.1 Model Description

Based on section 1.3.7 we followed [39] in writing a two-variable heat shock model,

$$\begin{aligned}\dot{y} &= U(y_t - y) - Rxy \\ \dot{x} &= -Ux + k(y - y_0)\end{aligned} \qquad \textbf{(4.3.1.1)}$$

Again, y are the unfolded (i.e. thermally denaturated) proteins, U is the thermal damage rate which is a non-linear function of the temperature. This temperature dependence is not explicitly considered here, R is the repair rate factor which gives the probability of y re-folding when colliding with x, a HSP. y_t stands for the proteome size (not including HSPs). These equations are linear and therefore you always get a solution where the steady state number of unfolded proteins is less than the total number of proteins, $y_{st} < y_t$. In other words, linear integral gain is too robust to allow for collapse (as illustrated in Fig. 4.1.1.2) to occur.

To allow for a bifurcation and a possibility of HSM failure we assume that in order for a x protein to be produced, two naturated proteins are needed. Indeed, this is a naive assumption, but it does make sense that in order for regulation to work the, cell has to be in reasonably good shape, and therefore the integral gain factor is some nonlinear function of $y_t - y$. As will be shown below, this extension is sufficient for a failure of the servo system to be possible. The set of equations is now,

$$\begin{aligned}\dot{y} &= U(y_t - y) - Rxy \\ \dot{x} &= -Ux + k(y_t - y)^2(y - y_0)\end{aligned} \qquad \textbf{(4.3.1.2)}$$

Notice the model is not fine-tuned with respect to the number of naturated proteins, i.e. the $(y_t - y)$'s power in the second equation. The choice of two is minimal and can be increased.

To see what the steady state solutions are, we equate the derivatives to zero which yields:

$$\begin{aligned}Rx_{st}y_{st} &= U(y_t - y_{st}) \\ Ux_{st} &= k(y_t - y_{st})^2(y_{st} - y_0)\end{aligned} \qquad \textbf{(4.3.1.3)}$$

Eq. 4.3.1.3 can then be further simplified to obtain:

$$\alpha(y_t - y_{st})^2(y_{st} - y_0)y_{st} = (y_t - y_{st}) \ , \alpha \equiv \frac{Rk}{U^2} \qquad \textbf{(4.3.1.4)}$$

Working with $R=1, \ \ k=1, \ \ y_t=10, y_0=0.1y_t$ we can plot both sides of equation 4.3.1.4 (referred to as 'LHS' and 'RHS') to get a graphical solution for different U values as illustrated in Fig. 4.3.1.1. The proposed model, 4.3.1.3, demonstrates 2 different regions, separated by a critical U value (i.e. a bifurcation point), $U_c \cong 11.2$. For $U < U_c$ we have 3 equilibrium points, two of which are stable - $y_{st} = y_t = 10$ corresponding to a dead cell, and $y_{st} \cong 3.8$ which represents a living cell. However, for $U > U_c$ only the dead solution is valid

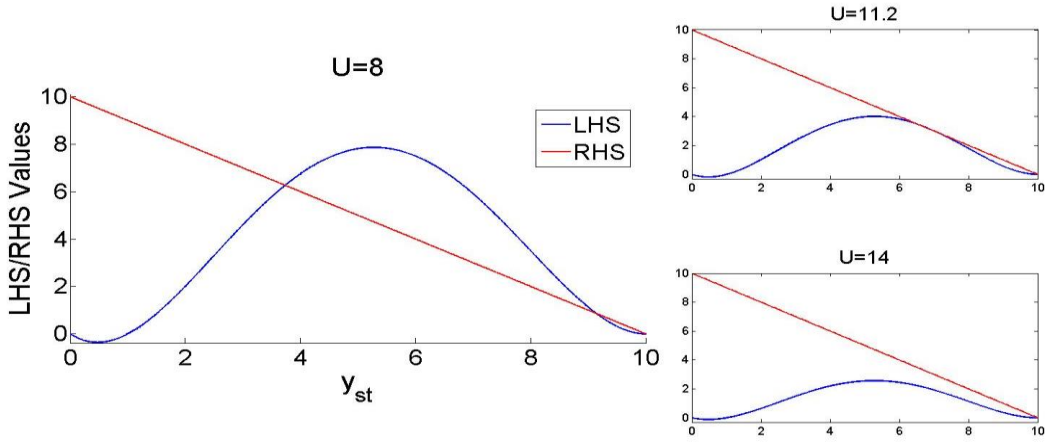

FIG 4.3.1.1 A graphical solution for y_{st}. ***(U=8)*** At the low U region two stable equilibrium points can be identified, separated by an unstable equilibrium point. The $y_{st} = y_t = 10$ equilibrium point (which corresponds to a dead cell) is valid for all temperatures, as expected. To the second stable equilibrium point ($y_{st} \cong 3.8$) we shall refer to as a live cell. In this low temperature regime, the viable equilibrium state is fine-tuned by the temperature, meaning that y_{sy}^{viable} shifts to lower values upon temperature decrease. ***(U=11.2)*** In this figure the two curves are tangential, which means the viable state sharply loses stability heralding the transition to a different dynamic regime. Thus, $U_c \cong 11.2$ is a bifurcation point. ***(U=14)*** High temperature region. Here we have only one stable state – that of a dead cell.

The model described above is already sufficient for the demonstration of life and death as stable attractors and the critical transition between them. However, the model 4.3.1.3 suggests we have a parameter range where the viable state is a stable equilibrium point, while in real systems we know that, eventually, the dead state is the only stable equilibrium point. Moreover, in our data we have observed two different types of viability decrease vs. time. At relatively high temperatures we have witnessed an exponential decay of viability vs. time. However, at temperatures of only 2-3^{0}C above the critical point we have witnessed a sigmoidal-like decrease in viability. This sigmoidal decrease could suggest the sudden exhaustion of resources needed for HSM. The long term exhaustion of resources may also account for the unstable nature of the live state. Such a mechanism would make sense since we work with a low concentration sample in water medium and the yeasts wear down due to the non-replenish nature of our system, lacking sugars, amino acids and other vital nutrients. All these essential substances we model by a single variable, z , to which we refer as 'energy', keeping in mind it is an effective variable which stands for more than just the narrow meaning of the word. Treating the 'energy molecules' as substrates, crucial to the well catalytic performance of enzymes, we modeled the functioning decrease due to energy depletion by a Michaelis-Menten like dependency: $\left(\frac{1}{1+\left(\frac{z_0}{z} \right)} \right)$, where z_0 is a half rate energy constant. Yet, we introduced another energetic constant, E , representing the energetic cost involved in the manufacture process of a single HSP, as well as the energy consumption in the refolding process, which we crudely assumed to be characterized by the same energetic coin.

We thus get,

$$\dot{y} = U(y_T - y) - Rxy \cdot \left(\frac{1}{1 + \left(\frac{z_0}{z} \right)} \right)$$

$$\dot{x} = -Ux + k(y_T - y)^2 \cdot (y - y_0) \cdot \left(\frac{1}{1 + \left(\frac{z_0}{z} \right)} \right) \qquad \textbf{(4.3.1.5)}$$

$$\dot{z} = -E\left(k(y_T - y)^2 \cdot (y - y_0) + Rxy\right) \cdot \left(\frac{1}{1 + \left(\frac{z_0}{z} \right)} \right)$$

The last equation we added describes the depletion of energy due to cell systems' functioning, in the absence of external energy source.

Since the data we collect is statistical in nature, to compare the model to the experiment stochasticity has to be added to the model. As a final step, we added a normal distributed noise to our system, yielding stochastic non-linear differential equations. The noise was introduced to the model upon each time step by multiplying each variable increment (dx, dy, dz) by an independent noise factor randomly chosen from a uniform distribution in the [0,1] interval . The results in the next section are averaged over 100 program runs. A viable cell was naively defined as one having at least 10% functioning proteins (i.e. $y < 0.9 \cdot y_t$).

4.3.2 A Qualitative Comparison between Model Results and Measurements

As indicated by the headline of this section, this part presents only qualitative comparison between the model and real data. Of course, the next step would be to feed real biological parameters to the model

The critical point in the numerical simulation was found to be $U_c \cong 30.5$. Let us first examine the hot temperatures regime (i.e. $U > U_c$): From the right graph in Fig. 4.3.2.1 we can learn that in hot temperatures the viability decay with time is exponential,

whereas, decay pattern becomes more sigmoidal in nature upon a temperature decrease. The numerical simulations show a similar behavior, though the low rate viability drift before the collapse is unique to the real data.

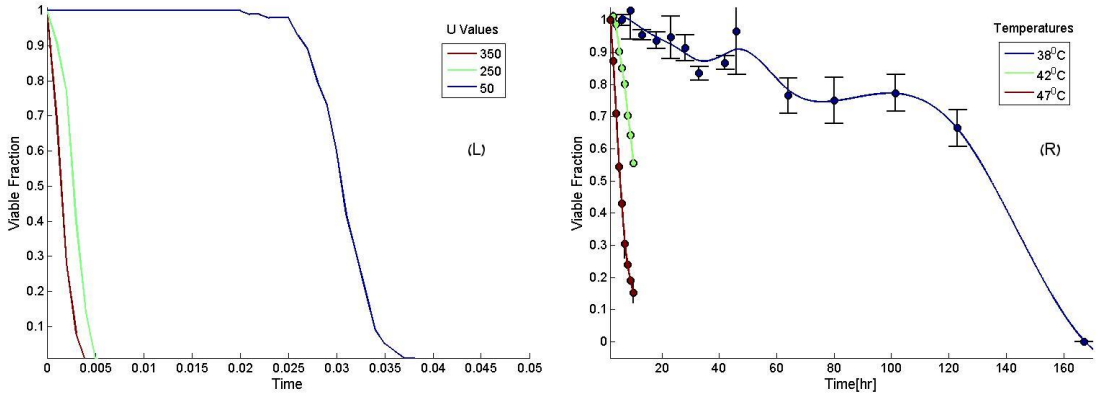

FIG 4.3.2.1 (L) A dynamic model for 3 'hot temperatures'. The bifurcation point in the model was pinpointed at $U_c \cong 30.5$, which places all the curves in the graph at the 'hot temperature' regime. (R) Real data. The values in this graph were normalized to start from 100% viability.

We can also compare viability vs. temperature profiles in various heating times (which is actually how we measure our system). In Fig. 4.3.2.2 the critical region is included in the temperature range. Looking at the right picture we can see that the sigmoidal trend we observed in Fig. 4.3.2.1-R becomes sharper upon temperature decrease, as predicted by the model.

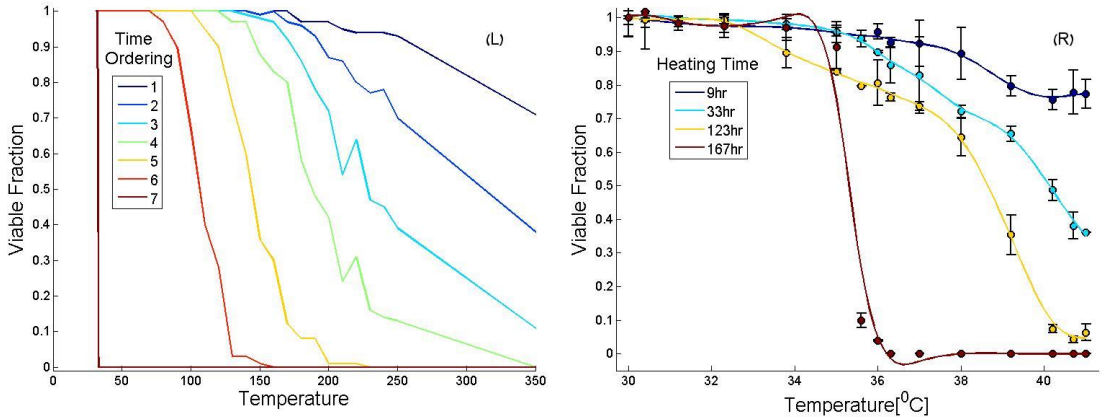

FIG 4.3.2.2 (L) Model dynamics for different heating times. A sigmoidal shaped collapse unveils as we draw nearer to the critical temperature; this trend stands in good agreement with actual measurements presented at (R). The values in the right graph were normalized to start from 100% viability.

As the critical temperature is approached energetic considerations become more important. When we examine viability levels in temperatures which are lower than the critical temperature (~ 30.5) we see a different kind of collapse, one that is driven by an interplay between energy depletion and protein misfolding (Fig. 4.3.2.3). Drawing closer to the critical temperature, time scales are substantially stretched (see Fig. 4.3.2.4), which in turn allows energy levels to start playing a significant role. Before this stretch (i.e. critical slowing down) energy levels stay almost constant (with respect to the z_0 scale).

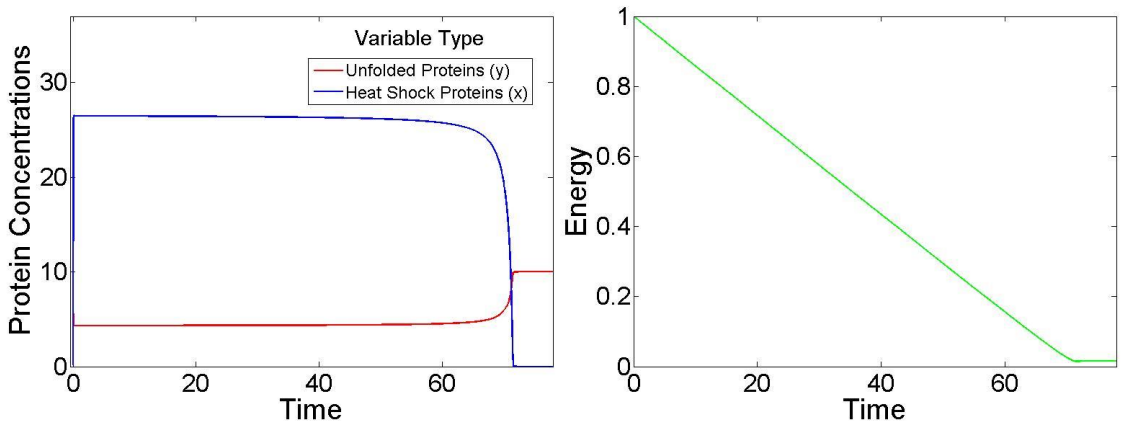

FIG 4.3.2.3 Energy depletion plays a crucial role at low temperatures, $U = 20$ .Despite linear energy depletion, Homeostasis is strictly maintained until $t \cong 70$ when the system rapidly collapses. The dynamics illustrated in this graph is typical to the low temperature regime, where critical slowing down allows time for energy depletion.

Lastly, we characterized (Fig. 4.3.2.4) the time stretch which appears as we tend to the critical point from the right (meaning from hot temperatures). Following section 4.1.2 we devised a power law fit to calculate the critical slowing down exponent.

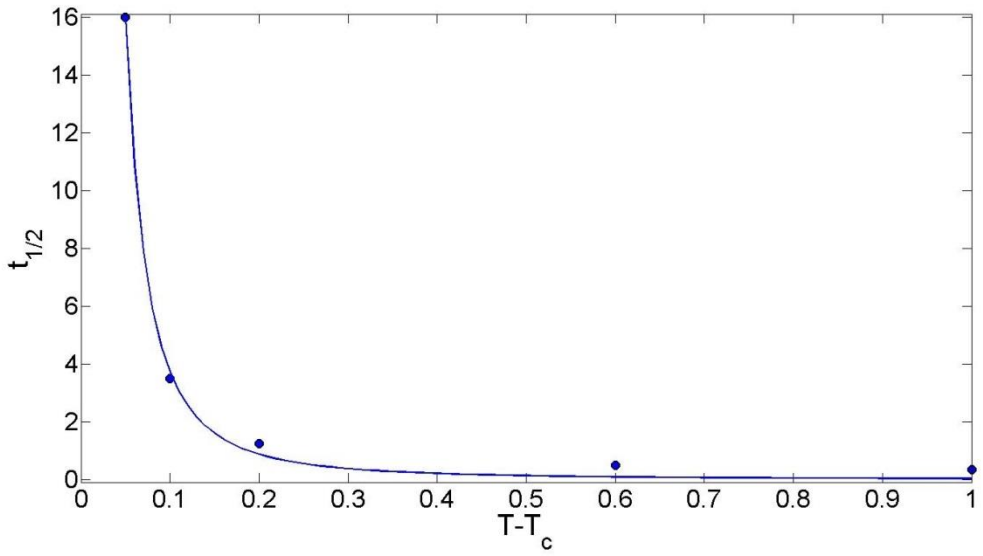

FIG 4.3.2.4 Critical slowing down – a power-law fit, $R^2 = 0.997$. The blue solid line is a maximum likelihood fit of a power law decay $t1/2 = a \cdot (T - Tc)^b$. We measure a critical exponent value of $b = -2.1$ $\left(-2.8,\ -1.4\right)$.This value is not robust as are all the other values involved with the suggested model.

Once we reach the low temperature regime ($U < U_c \cong 30.5$) we see a very moderate time dynamic, which marks this region as a 'non-thermal death' regime.

Another slowing down appears as we take $U \to 0$. However, this is not a critical slowing down, but a rather trivial stretching of time scales caused by the freezing of the physical time scale in our system.

5 Discussion

5.1 Cell death as a Critical Phenomenon

In the introduction we described how in critical systems a sharp collapse happens as a control parameter (i.e. temperature) is scanned across a certain critical value. Part 4.1.1 illustrated how continuous viability curves turn to a sharp sigmoidal-shaped decay, strongly supporting the relevance of critical phenomena to the thermal life-death transition of cells. Moreover, in part 4.3.2 we learned how a non-linear stochastic dynamic model can yield similar behavior. We are further encouraged by the slowing down of death rates as the critical temperature is approached, evident from Fig. 4.1.2.1. Indeed, the best fit was obtained under the assumption of power-law scaling, which was also the case with the dynamical model (Fig. 4.3.2.4).

Note that the observations presented in part 4.1.1 are preliminary and based on a single data set. These observations have to be re-confirmed in repetition experiments that are currently under way.

The existence of a critical point in parameter space, below which a cell would survive, but above which a cell will die with certainty after a sufficiently long time could be studied in the future as a sieve for the selective destruction of certain cell types given that their critical point is lower than the cells in their environment, with applications in cancer treatment as well as bacterial infection.

As explained in the introduction, measuring critical slowing down can do more than just imply the occurrence of critical behavior. Certain critical exponent values may suggest thermal cell death is a part of a specific universality class. A universality class points out the existence of a few salient features the members of the class share. It further suggests a joint effective dynamic model (i.e. a Hamiltonian) to which the systems in the class (whose specifics can in general be very different from one another) tend to as they approach a critical point (for further reading, see 6.1.2-3).

Remarkably, the critical exponent we measured, $\gamma = -1.23$ $(-1.49,-0.98)$, falls in the range of one of the main universality classes that was briefly mentioned in the

introduction. Since the universality class is defined by a critical exponent range of $1.2-1.3$, it is clear that the error in our measurements must be reduced if we wish to make a more definite statement. Altogether, universality classes may reveal an interesting course to apply the way systems are modeled in Physics (via Hamiltonians) to the cell system (for a broader view on the issue, please advise section 6.1 in the appendix part).

Several future research directions can follow this work:

The universal nature of death can be tested under various stress factors, using different organism models. It would be interesting to understand whether the critical exponent of slowing down is the same for different cell death mechanisms or not.

Moreover, applying various types of stress concurrently may reveal a more intricate seperatrix in multidimensional parameter space.

In our work we showed that a model that was originally devised to describe dynamics of variables inside the cell can be altered to describe a macroscopic transition from a viable state to a dead state. The model is consistent with experiment on the qualitative level, as a somewhat exponential decay turns to sigmoidal decay, with bifurcation and critical slowing down becoming apparent. The next step would be to fit real values to the various free parameters of the model and see if the model agrees with experiment results on the quantitative level as well.

Since we work with a statistical ensemble, a more direct modeling approach would invoke equations that describe distribution functions rather than real variables. The Fokker-Planck equation displays critical behavior [43], and is naturally driven by two forces - 'diffusive force' and 'drift force'. These two 'forces' give rise to two respective time scales. The 'diffusive' timescale may account for the non-thermal death rate evident from the data, while the 'drift' timescale may describe the thermal death rate.

From an experimental point of view, a more direct approach to characterizing cell death dynamics is identifying and measuring an order parameter (see section 6.1.1.1 in the appendix). A natural candidate [44, 45]to serve as one in our system is the 'percentage of

unfolded proteins' in the cell or any other quantity proportional to it. Of course, there could be more than one order parameter describing the life-death transition (i.e. membrane penetrability, transcriptional activity and more), adding further levels of complexity to the issue.

A currently running experiment (50 days long up to now) implies that slow thermal death continues at long heating times below 36^0C, and that another critical temperature is located at $T \cong 30^0 c$, with clear critical slowing down. Though results are still unripe, it seems that a sharp sigmoidal shaped collapse is evolving around $T \cong 30^0 C$ as well.

5.2 The Salvage Effect

The work conducted in this part of our research was mainly phenomenological, with relatively little effort aimed to explain the biologic origin of the phenomenon. It is clear that much work is left to be done in order to support an explicit biological explanation to this phenomenon, such as a more thorough work with stained and mutated strains.

In our study we characterize viability levels as we change two control parameters: heating time and temperature. We discovered that viability levels follow a non-monotonous pattern in different temperature regions. The pattern turned to be significant and reproducible in various experimental conditions as well as on different PCR and FACS machines. O.D recovery rates (4.2.3) and O.D levels during the heat shock (4.2.4) both supported the non-monotonous behavior evident from viable-dead post heating distributions. The salvage pattern (i.e. the peak in the viability graphs) seems to be a discrete phenomenon riding on a general exponential decay trend which describes the drop in half-life values as a function of temperature.

Measuring viability levels for a temperature gradient at different heating times reveals a dynamic salvage pattern (at least in the $[50,56]$ temperature range), as the maximal viability point drifts toward lower temperatures as heating time is increased.

In attempt to better understand the mechanism behind the salvage pattern we worked with the mutant cell, $\Delta msn2$. The salvage pattern was reconstructed in the $\Delta msn2$ case, though the peak's amplitude reduced by half as did the typical width of the effect (Fig.

4.2.5.1). This outcome points out the HSM plays a central role in the creation of the effect. Yet, the most surprising part of Fig. 4.2.5.1 lies in the deep preceding the salvage peak (41.7^0C-42.5^0C, heating for 14 hours); in this region the mutant cell performs better than the wild type which implies the heat shock system is overexpressed in this region. In this view, the deviation from monotonic behavior is not necessarily 'salvage' in nature but results from an overexpression of the heat shock system under certain conditions.

Another perspective is offered by the fact that working with water medium produced only monotonic behavior under all conditions. It is clear that since there is no cell proliferation in water the salvage in cell division disappears as well. A possible explanation could be that cell proliferation is by itself a recruited HSR. Cell division may raise viability levels as the process ends with a new cell that can better keep up with the prolonged heat stress. The mother cell may be doomed to die, since it not only had to deal with the heat stress, but also allocated substantial energy resources towards proliferation. This strategy may be beneficial in the long term since the system is left with one presumably dead mother cell and one fresh cell with a new heating clock. According to this approach cell division acts as a highly efficient HSM, since the defected proteins tend to stay within the mother cell. Cell division acts as a jackpot strategy for waste evacuation, though the price is obvious.

On one hand, when conditions are optimal, the cell systems work efficiently and cell division rates are the highest. On the other hand, following the logic of the suggested interpretation, more defects imply that the cell is prone to use cell division as a HSM. Superimposing two opposing monotonic phenomena may yield a peak in the resulting function. Moreover, this explanation seems to be consistent with OD recovery patterns we encountered in section 4.2.3: We can see that the recovery rate at 43.5^0C is slower, though we know that at 43.4^0C the OD levels were higher during the heat shock, with respect to 42°C (Fig. 4.2.4.2). In this view the exhaustion of the sample's proliferation capacity (at 43.4^0C) during the heat shock process has a price which is evident by the slow recovery rate.

6. Appendix

6.1 Critical Phenomena and 2nd Order Phase Transitions- A physical Approach

Before embarking on a more formal exposition of the theory of critical phenomena it is appropriate to ask what the main aim of the theory should be. This is sometimes held to be the calculation of the observable properties of a system from first principles. From a physical point of view, the aim of the theory of complex phenomenon should be to elucidate which general features of the Hamiltonian of the system lead to the most characteristic and typical observed properties, such as phase transitions and critical points.

In physics, critical phenomena are the collective name associated with the physics of critical points. Most of them stem from the divergence of the correlation length, but also the dynamics slows down, as described in the canoe case. Critical phenomena include scaling relations among different quantities, power-law divergences of some quantities (such as the magnetic susceptibility in the ferromagnetic phase transition) described by critical exponents, universality, fractal behavior, ergodicity breaking etc. Critical phenomena take place in second order phase transition, although not exclusively.

6.1.1 Phase Transitions and Critical Points

Change of phase, such as the boiling of water, is one of the most striking aspects of the macroscopic physical world. In many cases the various phases of matter seem quite dissimilar and separate, and transitions between them are abrupt and unheralded. More formally, those transitions in which one or more first derivatives of relevant thermodynamic potential change discontinuously as a function of their variables may be called *first-order transitions* (Ehrenfest classification) . For a fluid it is appropriate to consider the Gibbs free energy as a function of P and T .

On the other hand, transitions in which the first derivatives of the thermodynamic potential remain continuous, while only higher-order derivatives are divergent or change discontinuously at the transition point may conveniently be termed continuous transitions. All 2nd order phase transitions correspond to a symmetry change. It is for such

transitions that we use the term '*critical point*'. Some common examples for systems in which one can find 2nd-order phase transitions are (i) a binary fluid mixture; (ii) ferromagnet-paramagnet phase transition; (iii) various superconductivity and superfluidity related phenomena.

A dominant characteristic is the large increase of the microscopic fluctuations in the vicinity of a critical point which herald the approaching transition. These fluctuations can reach effectively macroscopic magnitudes as illustrated by the critical opalescence optical effect. Consequently, a problem of central interest in the study of critical phenomena is the determination of the asymptotic laws governing the approach to a critical point.

6.1.1.1 Order Parameter

Order parameter is a measure of the degree of order in our system. Briefly put, the order parameter is the number that indicates in which phase you are, and normally changes from zero to one across the critical point, and reflects the different symmetry of the system at both its sides. When a symmetry breaks, one needs to introduce extra variables to describe the state of the system. What the order parameter is depends on your system. For example, if you are looking at a ferromagnet, the order parameter would be the average magnetization (above the critical temperature the magnetization is random so the average is zero, below the critical temperature there is a clear preferred direction and the average will be non-zero); for a phase transition between liquid and gas the order parameter may be the difference in density between the phases. In many cases it is wise to identify the order parameter with the first derivative of the free energy with respect to an external field since it's continuous in 2nd order phase transitions [42].

6.1.2 Critical Exponents and Universality Classes

As we have previously mentioned various physical quantities diverge as some variable, e.g. temperature, approaches its critical-point value, it is appropriate to present a proper mathematical definition which enables critical behavior to be characterized numerically. We may say a function $f(x)$ varies as x^{λ} when x approaches zero from above, or we may write:

$$\lim_{x\to 0^+}\left(\frac{\ln f(x)}{\ln x}\right)=\lambda \qquad \textbf{(6.1.2.1)}$$

For example, for a gas-liquid system the critical point is characterized by the vanishing difference between the densities of gas and liquid phases. We define the exponent β by:

$$\rho_L-\rho_G\sim(T_c-T)^{\beta},\ \ T\to T_c^{\ -} \qquad \textbf{(6.1.2.2)}$$

From above, the critical point is most readily characterized by the divergence of the isothermal compressibility:

$$K_T\sim\frac{1}{(T_c-T)^{\gamma}},\ \ T\to T_c^{+},\ \ K_T\equiv-\frac{1}{v}\left(\frac{\partial v}{\partial p}\right)_T \qquad \textbf{(6.1.2.3)}$$

Every physical quantity may have its own exponent, but since the free energy is a function of two thermodynamic parameters, only two exponents are really independent. For example, γ also describes the divergence of a typical time scale in the system ($\tau\sim K_T$), a phenomenon to which we refer as *critical slowing down*.

Most simple gases obey the principle of corresponding states quite well, so values of $\gamma\cong 1.2-1.3$ turns out to be quite general. This suggests that the most salient features of the phase transition (e.g. critical exponents' values) do not depend sensitively on the details of the intermolecular interactions. Strikingly, this value range is not unique to a liquid-gas system, as can find exactly the same typical values when describing magnetic systems, binary fluids and alloys.

This intriguing phenomenon according to which critical exponents take the same values for very different physical systems is called *universality*. The different groups to which a bunch of physical systems are categorized are termed *universality classes*, and so one can pinpoint the DPD (directed percolation depinning) group, the QEW (quenched Edwards-Wilkinson) group etc.

6.1.3 Renormalization Group

The critical behavior is usually different from the mean-field approximation which is valid away from the phase transition, since the latter neglects correlations, which become increasingly important as the system approaches the critical point where the correlation length diverges. Lev Landau gave a phenomenological theory of 2^{nd} order phase transitions. Though historically important, we shall not review the details of Landau's theory. Instead, we shall set the stage for a mathematical apparatus called renormalization group (RG) which explains many qualitatively and also quantitatively properties of the critical behavior.

RG allows systematic investigation of the changes of a physical system as viewed at different distance scales. The RG is intimately related to "scale invariance" and "conformal invariance", symmetries in which a system appears the same at all scales (for further reading regarding the quantum field theory aspect of RG one may advice the classic introduction to quantum field theory by Peskin, chapter 13). As the scale varies and various degrees of freedom are dismissed (this RG step which is carried out repeatedly is termed *decimation*), it is as if one is changing the magnifying power of a microscope viewing the system. In renormalizable theories, the system at one scale will generally be seen to consist of self-similar copies of itself when viewed at a smaller scale, with different parameters describing the components of the system (this is the so-called *scaling hypothesis*). The parameters of the theory typically describe the interactions of the components. We identify a critical point with the fixed point of a RG flow (meaning, a convergence to specific parameters' values in the relevant parameter space of the system).

Consider a certain observable A of a physical system undergoing an RG transformation. The magnitude of the observable as the length scale of the system goes from small to large may be: (a) always increasing, (b) always decreasing or (c) other. In the first case, the observable is said to be a relevant observable; in the second, irrelevant and in the third, marginal.

A relevant operator is needed to describe the macroscopic behaviour of the system; an irrelevant observable is not. Marginal observables may or may not need to be taken into

account. A remarkable broad fact is that most observables are irrelevant, i.e., the macroscopic physics is dominated by only a few observables in most systems. As an example, in microscopic physics, to describe a system consisting of a mole of carbon-12 atoms we need of the order of 10^{23}(Avogadro's number) variables, while to describe it as a macroscopic system (12 grams of carbon-12) we only need a few.

Before the RG, there was an astonishing empirical fact to explain: the coincidence of the critical exponents (i.e.: the behaviour near a second order phase transition) in very disparate phenomena, such as magnetic systems, superfluid transition, alloy physics, etc. This was called universality and is now successfully explained by RG, just by showing that the differences between all those phenomena are, in fact, related to such irrelevant observables.

Thus, many macroscopic phenomena may be grouped into a small set of universality classes, specified by the set of relevant observables.

6.2 Critical Phenomena and Non-Linear Dynamics- A Mathematical Approach

Of course mathematicians have their own jargon with which they describe their view point on the subject. In order to keep things simple we shall use the terms we encountered in the last section when there is a well-defined correspondence between both terminologies.

6.2.1 A Short Introduction to Catastrophe Theory

Catastrophe theory is a mathematical program which attempts to study how the qualitative nature of the solutions of equations depends on the parameters that appear in the equations. We look for solutions, x_i for dynamical systems of n equations:

$$\dot{x}_i = f_i\left(x_j; c_\alpha; t\right) \qquad \textbf{(6.2.1.1)}$$

Where $x_i \in \Re$, and c_α stands for control parameters such as temperature, magnetic field etc.

We can simplify the situation by assuming f_i is time dependent. Moreover, if a potential V can be found, such that:

$$f_i = -\frac{\partial V(x_j; c_\alpha)}{\partial x_i}$$

Then we get a classical gradient system:

$$\dot{x}_i = -\frac{\partial V(x_j; c_\alpha)}{\partial x_i} \qquad \textbf{(6.2.1.2)}$$

Indeed, many physical systems can in fact be described by potentials depending on control parameters.

Of particular interest are the equilibria $\dot{x}_i = 0$ of dynamical and gradient systems. The equilibria $x_i(c_\alpha)$ of a gradient system are defined by the equation:

$$\frac{\partial V(x_j; c_\alpha)}{\partial x_i} = 0 \qquad \textbf{(6.2.1.3)}$$

Elementary Catastrophe Theory is the study of the equilibria of gradient systems, and how they depend on c_α .

To understand the basics' of critical phenomena we shall focus our discussion on the elementary theory.

6.2.2 The Local Character of Potentials

The local character of a potential is described by a sequence of theorems of functional analysis requiring an increasing intimacy with topology. We shall use the theorems for the sake of classification and ignore the specific details involved, as well as any cumbersome mathematic formalism.

6.2.2.1 The Implicit Function Form - Non-Equilibrium points

In the case of a non-zero force $F \equiv -\nabla V \neq 0$ it is possible to choose a new coordinate system in the neighborhood of this point so that the force has only one nonvanishing component:

$$\left\{\begin{array}{l} y_1 = y_1(x_1,...,x_n) \\ \quad\vdots \\ y_n = y_n(x_1,...,x_n) \end{array}\right. \xrightarrow{\text{In the new coordinates}} V = y_1 + \text{constant}$$

The constant term is not important when dealing with the local properties of a potential, and will further be dropped from consideration.

6.2.2.2 The Morse Forms- Equilibrium Point

If the physical system is in equilibrium, $\nabla V = 0$, the stability properties of the equilibrium may be determined from the eigenvalues of the Hessian matrix $V_{ij} = \dfrac{\partial^2 V}{\partial x_i \partial x_j}$.

If $\det(V_{ij}) \neq 0$ a theorem of Morse guarantees the existence of a smooth change of variables so that the potential can be written locally as a canonical quadratic form:

$$V = -y_1^2 - ... - y_i^2 + y_{i+1}^2 + ... + y_n^2$$

6.2.2.3 The Thom Forms- Critical Points

Since the potential's eigenvalues depend on the control parameters, one or more of the eigenvalues may assume the value zero for certain values of c_α, ending up in $\det(V_{ij}) = 0$. By definition, the equilibrium points of $V(x_1...x_n)$ at which $\det(V_{ij}) = 0$ are called critical points.

If l eigenvalues vanish at $c_\alpha = c_\alpha^0$, then the Thom Splitting Lemma may be used to split the potential into a non-Morse part and a Morse part:

$$V = Cat + \sum_{j=l+1}^{n} \lambda_j(c) y_j^2 \quad ; \quad where \quad Cat = CG + Pert \qquad \textbf{(6.2.2.3.1)}$$

Cat stands for the catastrophe function, which can by itself be decomposed into a sum of two functions: *CG* which is the catastrophe germ, and *Pert* which represents the perturbation. When $c_\alpha = c_\alpha^0$ the catastrophe function reduces to the catastrophe germ which is typically a power law function with respect to the relevant control parameters.

Who are now at the point where we can describe the mathematic equivalent of the physical universality classes we met at the previous section. Let us present a partial table of various 'mathematical classes' for different number of control parameters (denoted by k):

Table 6.2.2.3.1

Name	k	Germ	Perturbation
A_2	1	x^3	$a_1 x$
$A_{\pm 3}$	2	$\pm x^4$	$a_1 x + a_2 x^2$
A_4	3	x^5	$a_1 x + a_2 x^2 + a_3 x^3$
D_{-4}	3	$x^2 y - y^3$	$a_1 x + a_2 y + a_3 y^2$

Where a_i values are related to the physical control parameters.

I want to stress the interpretation of the germ function through the example of A_4: When we write $CG = x^5$ we actually mean that all the lower terms in $CG's$ Taylor's expansion vanished. Indeed, a certain choice of control parameters may cause these leading terms to vanish, which results in a qualitative change in the function's properties; the terms which remain (of which the new leading term is the most influential) determine the qualitative properties of the function at a point. This is why these terms are called the *germ of the function*.

The catastrophe germ occurs in conjugation with perturbation functions listed in the right-hand column of table 6.2.2.3.1. The reason this additional baggage is required for the Thom canonical form is that perturbations affect the qualitative of a function at a critical point. Nonetheless, we shall live it be as the main focus of our research is the catastrophe germ itself.

A question that may have come up since the beginning of this document is ‘’Why characterize the critical points when it is obvious that most of the points of an arbitrary family of functions are non-critical?’’. I believe that we are now at the point of addressing this question properly. From a mathematical perspective, it is the measure zero set that parametrizes functions with degenerate critical points which completely organizes the global qualitative properties of the family of functions (notice c is a vector of free parameters) [43]. This seperatrix in the control parameter space is called the *bifurcation set* (or simply, *bifurcation*) and is worked out in the following section.

6.2.3 Bifurcations and Attractors

Let us describe a simple, zero-dimensional, example of a bifurcation. We consider the A_2 potential described in table 6.2.2.3.1:

$$A_2 = \frac{1}{3}x^3 + ax \quad \overset{equilibrium\ points}{\rightarrow} \quad x_2 + a = 0 \quad \overset{critical\ points}{\rightarrow} \quad 2x = 0$$

Indeed, $a = 0$ is a zero-dimension seperatrix set as illustrated in Fig. 6.2.3.1:

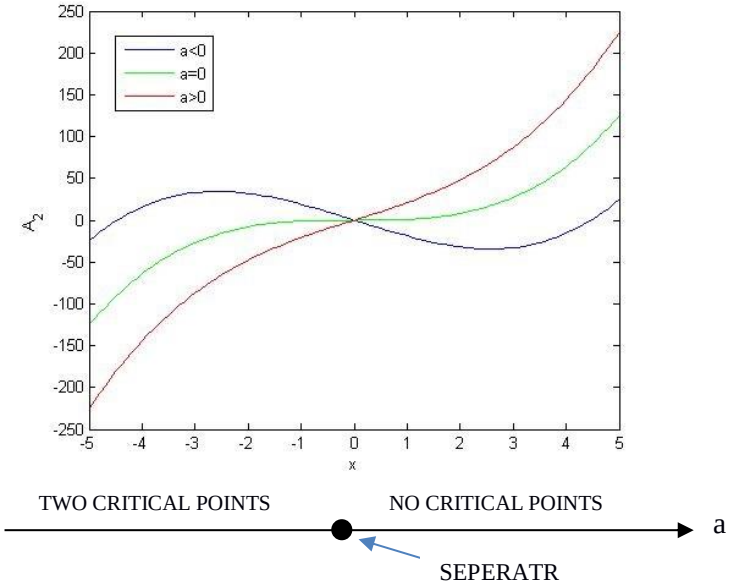

FIG 6.2.3.1 As we vary the control parameter's values from negative to positive we see a topological transition realized by the change in the number of critical points.

In the language of dynamical systems the minimum point we observe in the blue curve of Fig. 6.2.3.1 is called an *attractor*. More generally, an attractor is a set of physical properties toward which a system tends to evolve. One can think of the attractors as an effective potential land scape that controls the dynamics; heuristically speaking, if we pour water onto the potential land scape it will collect in lakes at the bottom of each valley. The minima around which the water gravitates are called attractors while watershed where the water collects is called a *basin of attraction*.

A bifurcation gets a simple interpretation within the attractors' terminology: The number of attractors in a non-linear dynamical system can change when a system parameter is changed; this change can be equivalently defined as a bifurcation. It is accompanied by a change of the stability of an attractor. More formally, in a bifurcation point, at least one eigenvalue of the Jacobian gets a zero real part.

To sum up, a bifurcation occurs when a small smooth change made to the parameter values of a system causes a sudden 'qualitative' or topological change in the behavior.

6.2.4 Catastrophe Flags

The presence of an elementary catastrophe can indeed be recognized by the occurrence of a critical point. However, such a point may not be recognized immediately for one reason or another. For example, (1) the potential may be a very complicated function or (2) it may not even be known accurately. Worse yet, (3) the system may not even be a gradient system, or (4) we may even not have the foggiest idea of the equations that describe the system properly. Nonetheless, catastrophes do have characteristic finger-prints to gain our attention, some of which are worth to point out:

1. **Modality**

This means that the system has two or more distinct physical states in which it may occur. In other words, the potential describing the system has more than one local minimum for some range of the external control parameters.

2. **Inaccessibility**

This means that the system has an equilibrium state which is unstable, since infinitesimal perturbations exist which decrease the value of the potential.

3. **Sudden Jumps**

This feature is inherently related to the bifurcations described in the last section. A small change in the value of the control parameter may result in a large change in the value of the state variable, as the system jumps from one local minimum to another. In a noisy environment, this sudden jump is accompanied by a smooth but nondifferentiable change in the value of the potential. The change in the value of the state variable often occurs on a fairly rapid time scale.

4. **Divergence**

A finite change in the value of the control parameters leads to a finite change in the equilibrium value of the state variables. Usually a small perturbation in the initial values of the control parameters will lead to only a small change in the initial and final values of the state variables. However, in the neighborhood of a critical point, small changes in the control parameter initial values may lead to large changes in the state variable final values.

5. Hysteresis

Hysteresis occurs whenever a physical process is not strictly reversible. That is, the jump from local minimum 1 to local minimum 2 does not occur over the same point in control parameter space as the reciprocal jump from local minimum 2 to local minimum 1.

6. Divergence of Linear response

Under a slight change in the values of the control parameters $\left(c \to c^0 + \delta c^0\right)$ the location of an equilibrium will typically move slightly $\left(x \to x^0 + \delta x^0\right)$. The linear response of δx_j^0 to δc_α^0 is given through the susceptibility tensor:

$$\delta x_j^0 = \chi_{j\alpha}\left(x^0; c^0\right)\delta c_\alpha^0$$

As the equilibrium approaches a critical point $\chi_{j\alpha}$ becomes exceedingly large, until it diverges at the point.

7. Anomalous variance

A physical system may be defined by a probability $P(x)$ defined over the relevant phase space. Such a system is characterized by the moments of the probability distribution function, the second of which is the variance:

$$\left\langle x_i x_j \right\rangle = \int x_i x_j P(x) dx$$

It turns out that in the neighborhood of a critical point the variance may become large (''anomalous'').

8. Critical Slowing Down

As a system approaches a bifurcation, the time needed to recover from perturbations becomes longer and hence the system becomes more correlated with its past. Let us examine how this phenomenon manifests itself in a gradient dynamical system:

$$\dot{x}_i = -\frac{dV}{dx_i}$$

If $\left(x^0; c^0\right)$ is an equilibrium, then

$$V(x;c) = const. + \frac{1}{2}\delta x_i \delta x_j V_{ij} + \mathrm{O}(3)$$

The equations of motion in the neighborhood of the equilibrium are:

$$\dot{x}_i = -V_{ij}\delta x_j + \mathrm{O}(2)$$

By neglecting the terms of 2nd order, the dynamical equations reduce to a simple system of linear equations. As the bifurcation set is approached, $\det(V_{ij}) \to 0$ so that one or more of the eigenvalues approaches zero. The relaxation time of the corresponding mode becomes larger and larger. That is, as we approach critical point, it becomes more and more difficult for (at least) one of the modes to relax back to zero. This lengthening of the relaxation time scale is called *critical slowing down*.

6.2.5 The Importance of Critical Points from a Mathematical Point of View

Once one of these catastrophe flags has suggested the presence of a catastrophe, the control parameters may be varied in a search for the relevant remaining flags. The other will occur under suitable conditions. The location of the catastrophe will often provide, at low cost, an enormous amount of information about the description of the physical system. The presence and type of catastrophe could suggest:

1. A simplified model potential depending on only the appropriate state variables and control parameters; or
2. The appropriate germ of a potential which , in turn, could suggest the physical process that is actually occurring; or
3. Indicate the appropriate type of equations (dynamical, diffusive, etc.) for the system; or
4. Dispense with the need for equations altogether, if the inferences to be drawn from such equations depends primarily on the canonical geometry of the associated catastrophe.

Although catastrophes arise from the qualitative study of equations, we can sometimes determine qualitative consequences even if we don't know the equations, provided we recognize the presence and type of catastrophe.

7. Literature

[1] **M. Scheffer** et al., Nature 461, 53 (2009).

[2] **T. M. Lenton**, Nat. Clim. Change 1, 201 (2011).

[3] **S. R. Carpenter, W. A. Brock**, Ecol. Lett. 9, 311 (2006).

[4] **E. H. van Nes, M. Scheffer**, Am. Nat. 169, 738 (2007).

[5] **J. M. Drake, B. D. Griffen**, Nature 467, 456 (2010).

[6] **S. R. Carpenter** et al., Science 332, 1079 (2011).

[7] **V. Dakos** et al., Proc. Natl. Acad. Sci. U.S.A. 105, 14308 (2008).

[8] **A. Hastings, D. B. Wysham**, Ecol. Lett. 13, 464 (2010).

[9] **Lei Dai, Daan Vorselen, Kirill S. Korolev, Jeff Gore**, Generic Indicators for Loss of Resilience Before a Tipping Point Leading to Population Collapse, *Science* 336, 1175 (2012)

[10] **S. H. Strogatz**, Nonlinear Dynamics and Chaos: With Applications to Physics, Biology, Chemistry, and Engineering (Westview, Boulder, CO, 1994).

[11] **C. Wissel**, Oecologia 65, 101 (1984).

[12] **Paris S, Pringle JR.** 1983. *Saccharomyces cerevisiae*: heat and gluculase sensitivities of starved cells. Ann. Microbiol. 134B:379 –385.

[13] **Singer MA, Lindquist S.** 1998. Multiple effects of trehalose on protein folding in vitro and in vivo. Mol. Cell **1**:639–648.

[14] **Singer MA, Lindquist S.** 1998. Thermotolerance in *Saccharomyces cerevisiae*: the Yin and Yang of trehalose. Trends Biotechnol. 16:460–468.

[15] **Elliott B, Haltiwanger RS, Futcher B.** 1996. Synergy between trehalose and Hsp104 for thermotolerance in *Saccharomyces cerevisiae*. Genetics 144:923–933.

[16] **Sanchez Y, Lindquist SL.** 1990. HSP104 required for induced thermotolerance. Science 248:1112–1115.

[17] **Kerscher O, Felberbaum R, Hochstrasser M.** 2006. Modification of proteins by ubiquitin and ubiquitin-like proteins. Annu. Rev. Cell Dev. Biol. 22:159 –180.

[18] **Bagola K, Sommer T.** 2008. Protein quality control: on IPODs and other JUNQ. Curr. Biol. 18:R1019 –R1021.

[19] **Requena JR, Chao CC, Levine RL, Stadtman ER.** 2001. Glutamic and aminoadipic semialdehydes are the main carbonyl products of metalcatalyzed oxidation of proteins. Proc. Natl. Acad. Sci. U. S. A. 98:69 –74.

[20] **Aguilaniu H, Gustafsson L, Rigoulet M, Nystrom T.** 2003. Asymmetric inheritance of oxidatively damaged proteins during cytokinesis. Science 299:1751–1753.

[21] **Causton HC, et al.** 2001. Remodeling of yeast genome expression in response to environmental changes. Mol. Biol. Cell 12:323–337.

[22] **Gasch AP, et al.** 2000. Genomic expression programs in the response of yeast cells to environmental changes. Mol. Biol. Cell 11:4241– 4257.

[23] **Giaever G, et al.** 2002. Functional profiling of the *Saccharomyces cerevisiae* genome. Nature 418:387–391.

[24] **Berry DB, Gasch AP.** 2008. Stress-activated genomic expression changes serve a preparative role for impending stress in yeast. Mol. Biol. Cell 19:4580–4587.

[25] **Lindquist S.** 1980. Varying patterns of protein synthesis in *Drosophila* during heat shock: implications for regulation. Dev. Biol. **77**:463– 479.

[26] **Kobayashi N, McEntee K.** 1990. Evidence for a heat shock transcription factor-independent mechanism for heat shock induction of transcription in *Saccharomyces cerevisiae.* Proc. Natl. Acad. Sci. U. S. A. 87:6550–6554.

[27] **Wieser R, et al.** 1991. Heat shock factor-independent heat control of transcription of the *CTT1* gene encoding the cytosolic catalase T of *Saccharomyces cerevisiae.* J. Biol. Chem. 266:12406 –12411.

[28] **Schmitt AP, McEntee K.** 1996. Msn2p, a zinc finger DNA-binding protein, is the transcriptional activator of the multistress response in *Saccharomyces cerevisiae.* Proc. Natl. Acad. Sci. U. S. A. 93:5777–5782.

[29] **Estruch F, Carlson M.** 1993. Two homologous zinc finger genes identified by multicopy suppression in a *SNF1* protein kinase mutant of *Saccharomyces cerevisiae.* Mol. Cell. Biol. 13:3872–3881.

[30] **Martinez-Pastor MT, et al.** 1996. The *Saccharomyces cerevisiae* zinc finger proteins Msn2p and Msn4p are required for transcriptional induction through the stress response element (STRE). EMBO J. 15:2227–2235.

[31] **Gross C, Watson K.** 1998. Transcriptional and translational regulation of major heat shock proteins and patterns of trehalose mobilization during hyperthermic recovery in repressed and derepressed *Saccharomyces cerevisiae.* Can. J. Microbiol. 44:341–350.

[32] **Frydman J.** 2001. Folding of newly translated proteins in vivo: the role of molecular chaperones. Annu. Rev. Biochem. 70:603– 647.

[33] **Ellis J.** 1987. Proteins as molecular chaperones. Nature 328:378 –379.

[34] **Craig EA, Gambill BD, Nelson RJ.** 1993. Heat shock proteins: molecular chaperones of protein biogenesis. Microbiol. Rev. 57:402– 414.

[35] **Lindquist S, Kim G.** 1996. Heat-shock protein 104 expression is sufficient for thermotolerance in yeast. Proc. Natl. Acad. Sci. U. S. A. 93:5301–5306.

[36] **Sanchez Y, Taulien J, Borkovich KA, Lindquist S.** 1992. Hsp104 is required for tolerance to many forms of stress. EMBO J. 11:2357–2364.

[37] **El Samad H, Goff JP, Khammash M,** (2002) Calcium Homeostasis and Parturient Hypocalcemia: An InCtegral Feedback Perspective. Journal of Theoretical Biology 214: 17–29. doi:10.1006/jtbi.2001.2422.

[38] **El-Samad H, Kurata H, Doyle JC, Gross CA**, Khammash M (2005) Surviving heat shock: Control strategies for robustness and performance. PNAS 102: 2736–2741. doi:10.1073/pnas.0403510102.

[39] **Pablo Szekely, Hila Sheftel, Avi Mayo, Uri Alon** , Evolutionary Tradeoffs between Economy and Effectiveness in Biological Homeostasis Systems, PLoS Comput Biol 9(8): e1003163. doi:10.1371/journal.pcbi.1003163, Published August 8, 2013

[40] Critical Transitions in Nature and Society, a book by **Marten Scheffer**.

[41] **Kenneth H.Jones and James A. Senft**, an improved method to determine cell viability by simultaneous staining with fluorescein diacetate- propidium iodide, The journal of Histochemistry and Cytochemistry, Vol. 33, No. 1, pp. 77-79, 1985.

[42] The theory of equilibrium critical phenomena, by **M. E, Fisher**.

[43] Catastrophe Theory for Scientists and Engineers, a book by **Robert Gilmore**.

[44] **Ken A. Dill, Kingshuk Ghosh and Jeremy D. Schmit**, Physical limits of cells and proteomes, Inaugural article (2011).

[45] **Barnett Rosenberg, Gabor Kemeny, Robert C. Switzer & Thomas C. Hamilton**, Quantitative Evidence for Protein Denaturation as the Cause of Thermal Death, *Nature* 232, 471 - 473 (13 August 1971); doi:10.1038/232471a0

[46] **J van der Zee**, Heating the patient: a promising approach?, a review, Annals of Oncology 13: 1173-1184, 2002, DOI: 10.1093/annonc/mdf280.

[47] **Van Uden** et. al. Archiv fur Mikrobiologie 61, 381 (1968)

[48] **Moats, J. Bacteriol**. 105, 165 (1971)